UNIVERSITY OF TENNESSEE HEALTH SCIENCE CENTER

MASTER OF SCIENCE THESIS

Iatrogenic Electrocautery Damage and Cellular-Based Corrosion of Total Joint Arthroplasty Biomaterials

---

Author:
Kirsten Carol Miller

Advisor:
William M. Mihalko, PhD

A Thesis Presented for The Graduate Studies Council of
The University of Tennessee Health Science Center
in Partial Fulfillment of the Requirements for the
Master of Science degree
In the Joint Graduate Program in Biomedical Engineering
From The University of Tennessee
And The University of Memphis

in

Biomedical Engineering: Biomaterials & Regenerative Technology
College of Graduate Health Sciences

July 2021

DEDICATION

I would like to dedicate this work to my amazing family and friends who have always been there to support and encourage me along the way. To my parents, Michael and Charlene Miller, for their unceasing love and patience. Without you, I would not be where I am today. To Cheyenne Rhodes, for always providing encouragement, having an open ear, and making Memphis feel like home. To my dear friends, Luke and Alanna Davis, for always being a source of laughter and comfort. To the dogs in my life, Skye and the "Boys", for always being a welcome distraction and source of glee.

ACKNOWLEDGEMENTS

I would like to thank my advisor, Dr. William M. Mihalko, for giving me the opportunity to pursue a graduate degree in Biomedical Engineering. Thank you for welcoming me into the program and continually lending me your guidance. I would also like to thank my committee members, Dr. Richard Smith and Dr. Erno Lindner, for their guidance, support and feedback.

I would like to thank Dr. Denis Diangelo, for always having an open office door to my many questions. I would like to thank Brian Marrow for lending me his time and teaching me how to use the profilometer, scanning electron microscopy, and energy dispersion x-ray spectroscopy equipment.

Additionally, I would like to thank and acknowledge my classmates who have been a source of support the past two years. Zoe Harrison, thank you for always being a source of encouragement and for lending an open ear to my worries. Alexis Nelson, thank you for being my get-stuff-done partner. Your positivity and kindness made all the studying and the hard work seem fun and enjoyable; our work sessions definitely kept me going this past year. Perri Johnson Jr., thank you for always checking up on me and encouraging me to keep going. Lastly, I would like to thank Ms. Shaquetta Barksdale. Our conversations at your desk never failed to make me smile and feel at ease.

Finally, I would like to thank my dear friends Kristin Cordell, Caroline Little, Courtney Lasher, Aubrey Pate and Madeline Sinclair. Thank you for always being one phone call or text away when times seem rough. Thank you for being sources of laughter, encouragement, and inspiration.

ABSTRACT

Introduction. The number of patients undergoing a Primary Total Knee Arthroplasty (PTKA) has been increasing steadily each year. Of those PTKA patients, 20% report long-term pain and/or some functional deficit. Cobalt-Chromium-Molybdenum (CoCrMo) alloy is one of the most used materials in Total Joint Arthroplasty (TJA) implants due the material's high strength, high corrosion resistance, and biocompatibility. The release of metal ions and potential occurrence of metallosis in TJA has been shown to be detrimental to the longevity of the implant. The mechanisms leading to this increase in metal ion concentrations have been up for debate, with some believing it is caused by Electrocautery (EC) damage at the time of surgery and others believing it is caused by inflammatory cells attacking the implant surface. The purpose of this thesis is to identify to what degree Electrocautery damage can alter the implant surface and if inflammatory cells are able to alter the implant surface and ingest metal particles.

Methodology. To better understand how EC damage can alter implant surfaces, three different types of femoral component bearing surfaces were selected and intentionally damaged in the operating room using the plasma arc from both monopolar (MP) (Bovie) and Bipolar (BP) (Aquamantys) sources. MP and BP EC damage was done at varying power levels using a 3-second hover method 3 mm from the implant surface. Scanning electron microscopy (SEM) was used to obtain a detailed microscopic analysis of the damaged areas. Energy-dispersive X-ray spectrometry (EDS) was utilized to assess the elements present in pits found in the corroded areas. Surface Topography was analyzed using a profilometer in the central portion of the damaged area for each MP and BP energy setting. Each damaged area was evaluated with the aid of TalyMap using ISO 4287 measurements for Arithmetic Average height (Ra), Kurtosis (Rk), Heighest Peak to Lowest Valley (Rz), and Skewness (Rsk). SEM, EDS, and Surface Topography were also used to look at undamaged areas of the implants.

In a separate experiment, IC-21 ATCC murine peritoneal macrophages were cultured with RPMI 1640 growth medium of supplemented with 10% fetal bovine serum (FBS), L-glutamine, and gentamicin. Select groups of cells were then activated using Interferon Gamma (IFNγ) and Lipopolysaccharide (LPS). CoCrMo alloy disks were cut, polished, passivated, and placed into 96 well plates and a select number intentionally damaged in the operating room with a MP EC device. After the cells were allowed to attach to the surface for 24 hours, culture medium was replaced every 12 hours and supernatant fluid was collected every 4 days starting on the second day of the experiment. After 30 days, cells were removed from the surface, counted and digested. The metal concentrations found in the supernatant and digested cell mixture were assessed using inductively coupled plasma spectrometry (ICP-MS), conducted at Brooks Applied Labs (Bothwell, WA). Statistical analysis was conducted using SigmaPlot and Microsoft Excel.

Results. Surface Profilometry quantified the topographical changes due to the damage form the MP and BP EC devices. The median R_a and R_z measurements were larger for the BP damaged areas compared to the MP for all bearing surfaces. The Oxinium surface

displayed the greatest increase in roughness parameters compared to the undamaged regions. The CoCr surface displayed the greatest R_{sk} for the BP damaged areas. The ZrN had the smallest differences in R_z and R_a for both MP and BP damage areas compared to undamaged areas. SEM imaging displayed pitting in the regions intentionally damage with a MP or BP EC device. Backscatter EDS analysis found significant changes in the elemental profile for the BP damage compared to the MP damage.

Cellular corrosion of the CoCr disks was quantified by measuring the concentration of Co, Cr, and Mo in the supernatant fluid collected off of the culture over the course of the 30-day experiment. The Co supernatant concentration was higher in the Undamaged Disks with Activated Cells versus its control which contained medium with no cells. The Cr concentration was higher in the supernatant fluid of the EC Damaged Disks with Standard Cells versus its control which contained medium with no cells. Between experimental groups, higher concentrations of Co and Mo was found in the supernatant of the Undamaged Disks with Standard Cells versus the EC Damaged Disks with Standard Cells. There was also a higher Co supernatant metal concentration when comparing the Undamaged Disks with Activated Cells versus the EC Damaged Disks with Activated Cells. A higher Cr supernatant metal concentration was found in the EC Damaged Disks with Activated Cells versus the EC Damaged Disks with Standard Cells. Following the end of the 30-day experiment, cells were digested to determine their inner metal ion concentration. There was a significantly higher intracellular Co and Mo concentration in the Undamaged Disks with Activated Cells versus the Undamaged Disks with Standard Cells. As well as a higher intracellular Co concentration in the EC Damaged Disks with Activated Cells versus the EC Damaged Disks with Standard Cells. SEM imaging displayed microscopic pitting on the surface exposed to macrophages and EC damage. Backscatter EDS analysis found significant differences in the elemental concentration of Carbon, Oxygen, Iron and Nickel between the experimental groups. From the EDS Backscatter analysis, the disks with EC damage displayed a higher Fe/C ratio compared to the undamaged disks. Showing evidence that EC damage alters the chemical profile of the CoCr disk surface.

TABLE OF CONTENTS

LIST OF TABLES

LIST OF FIGURES

LIST OF ABBREVIATIONS

ALTR	Adverse Local Tissue Reactions
ALVAL	Aseptic Lymphocyte-Dominated Vasculitis-Associated Lesions
BP	Bipolar
CoCrMo	Cobalt-Chromium-Molybdenum
EC	Electrocautery
ECIC	Electrocautery-Induced Corrosion
EDS	Energy Dispersion X-ray Spectroscopy
ICIC	Inflammatory Cell-Induced Corrosion
ICP-MS	Inductively Coupled Plasma Spectrometry
ICP-QQQ-MS	Inductively Coupled Triple Quadrupole Mass Spectrometry
IFNγ	Interferon Gamma
LPS	Lipopolysaccharide
MACC	Mechanically Assisted Crevice Corrosion
MOM	Metal-On-Metal
MP	Monopolar
NIH	National Institute of Health
PTHA	Primary Total Hip Arthroplasty
PTKA	Primary Total Knee Arthroplasty
R_a	Arithmetic Average Height Parameter
R_k	Kurtosis
R_{sk}	Skewness
ROS	Reactive Oxygen Species
RTHA	Revision Total Hip Arthroplasty
RTKA	Revision Total Knee Arthroplasty
R_z	Maximal Distance between Highest Peak and Lowest Valley
SEM	Scanning Electron Microscopy
THA	Total Hip Arthroplasty
TKA	Total Knee Arthroplasty
TJA	Total Joint Arthroplasty
ZrN	Zirconium Nitride

CHAPTER 1. INTRODUCTION

Significance of Research

Total Joint Arthroplasty (TJA) has become an extremely common procedure for those suffering from end stage osteoarthritis and rheumatoid arthritis. Total Knee Arthroplasty (TKA) procedures are projected to increase each year to an annual volume of 1.37 million by 2020 and 3.48 million by 2030 [1]. Of those patients that undergo TKA, about 15-20% of patients report unsatisfactory results following surgery compared to their expectations and up to 20% of patients report long-term pain and/or functional deficit post-surgery. Etiologies of failure in TKA patients include aseptic loosening, infection, instability, periprosthetic fracture, arthrofibrosis, polyethylene wear, suboptimal alignment of the implant and extensor mechanism deficiency [2-4].

TJA implants typically consist of cobalt-chromium-molybdenum (CoCrMo) and titanium alloy due to their excellent mechanical, corrosion, and biocompatibility properties [5]. While implant designs have been investigated to determine and implement methods of reducing the degradation caused by mechanical motion, other methods of corrosion have not been investigated in depth.

The occurrence and causes of implant alloy oxide layer damage have been investigated through basic science and implant retrieval studies. However, the discussion of whether this oxide layer damage is due to fretting, inflammatory cells, or electrocautery damage from surgeons continues. Discrepancies in the percentage of ICIC present in various retrieval studies (17 % from necropsy retrievals compared to 59% in revision surgery retrievals) provide evidence for disputes between the causes, occurrence, and clinical significance of inflammatory cell-induced corrosion (ICIC) and Electrocautery-Induced Corrosion (ECIC) [6, 7].

Orthopaedic Implant Alloys

To understand why certain metal alloys are used in a variety of medical applications (including Orthopaedic, Maxillofacial, Otolaryngology, Plastic and Neurosurgery), it is important to understand what encompasses a “biomaterial” and what can be stated as having “biocompatibility”. A biomaterial is defined as “a material designed to take a form that can direct, through interactions with living systems, the course of any therapeutic or diagnostic procedure” [8]. While biocompatibility is defined as “the ability of a material to perform its desired functions with respect to a medical therapy, to induce an appropriate host response in a specific application and to interact with living systems without having any risk of injury, toxicity, or rejection by the immune system and undesirable or inappropriate local or systemic effects” [9]. A biomaterial is determined as biocompatible by specific characteristics such as carcinogenicity, foreign body capsule response, hemocompatibility, host response, mineralization, osteoconduction, osteogenesis, osteoinduction, and thrombogenicity. The

goal of an implantable biomaterial in bone would be to have an appropriate host response and promote osteoconduction and osteoinduction.

Commonly used metal alloys in orthopaedic joint replacement applications include Titanium alloy (Ti6Al4V) and Cobalt-Chromium Alloy (CoCrMo). The use of these metal alloys for application in TJA has been focused on maximizing mechanical properties such as fatigue strength, creep strength, toughness, and wear resistance while also promoting long-term integration into the host environment [10]. However, the biocompatibility of these metal alloys is reliant on their corrosion rates when introduced to host dependent variables such as pH, oxygen potential, mechanical stress, and biological response to corrosion products. The combination of mechanical and electrochemical factors on orthopaedic metal alloys contributes to Mechanically Assisted Crevice Corrosion (MACC) of the implant. MACC encompasses fretting corrosion, corrosion fatigue, wear-assisted corrosion, stress-assisted corrosion, and stress-corrosion cracking [5]. The presence of MACC in TJA has been associated with adverse local tissue reactions and TJA revision.

The generated wear debris from MACC can be in the form of soluble ions or insoluble particles. Inflammatory cells recognize these wear particles as foreign objects and undergo phagocytosis when the size of the wear particles are from 150-nm to 10-µm in diameter [11].

Biological Response to Wear Debris

Generally, the materials used in orthopaedic implants are relatively biocompatible. However, these implants are subjected to high amounts of cyclic loading during normal use resulting in the production of wear debris. One of the main biocompatibility concerns of TJA implants is metal ion release into the local environment and also into the systemic circulation or lymphatic system. Therefore, it is important to understand how the host system reacts to the presence of the implant, wear, and corrosion products. Metal ion release from TJA implants has been seen to cause a plethora of adverse biological responses including local inflammation, cytotoxicity, hypersensitivity, and genotoxicity [12]. However, how the corrosion mechanisms resulting in this metal ion release alter implant surfaces is not well understood.

Local Effects of Implant Debris

The presence of implant metal debris has been seen to induce a local innate immune response through the activation of inflammatory cells such as macrophages, osteoclasts, and osteoblasts [13]. The activation of these inflammatory cells by the innate immune system initiates a release of inflammatory cytokines and chemokines (**Figure 1-1**). Macrophages and osteoclasts have been observed to phagocytose a range of ceramic, polymeric, and metallic wear debris and have been associated in aseptic loosening which is responsible for more than 44% of TKA revisions [13]. Macrophages

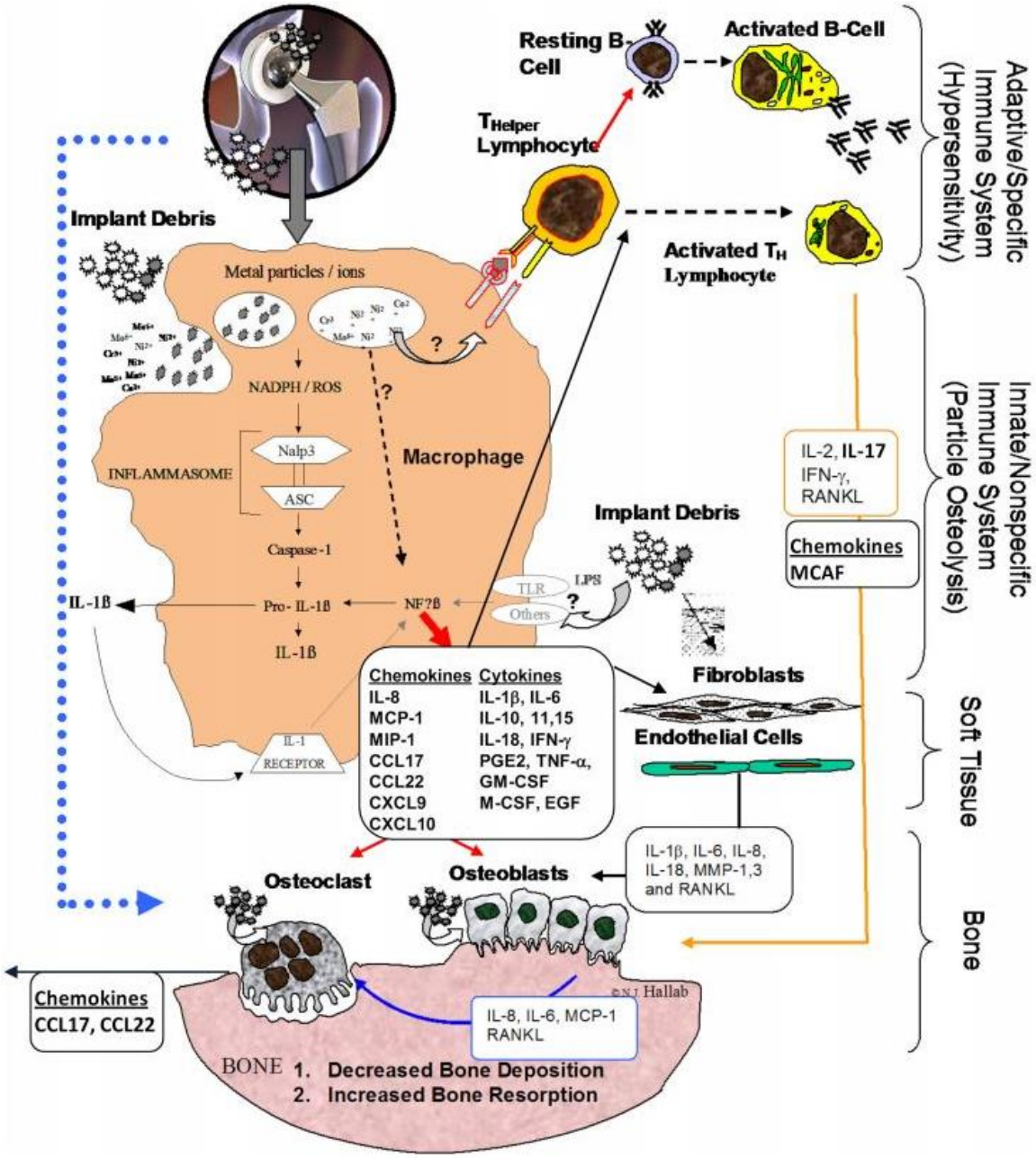

Figure 1-1. Signaling Schematic of the Innate Immune Response to Implant Debris-Induced Local Inflammation

Reprinted with open access permission. Hallab NJ, Jacobs JJ. Chemokines associated with pathologic responses to orthopedic implant debris. Frontiers in endocrinology. 2017 Jan 19;8:5 [14].

specifically have been seen to react to implant debris by releasing several M1 cytokines including interleukins (IL-1α, IL-1β, IL-6, IL-10, IL-11, and IL-15) and tumor necrosis factor α (TNF-α). As well as chemokines IL-8, monocyte chemotactic protein-1 (MCP-1), and macrophage inflammatory protein-1α (MIP-1α) [13-15].

Release of proinflammatory cytokines TNF-α, IL-1β, and IL-6 lead osteoblasts to produce receptor activator of nuclear factor-κB ligand (RANKL). The rupregulation of RANKL from osteoblasts allows for the binding of RANKL to osteoclast RANK receptors, thereby stimulating osteoclastogenesis leading to an increase in bone resorption [13]. Osteoprotegerin (OPG) is also released by osteoblasts to act as decoy receptors to control the number of osteoclasts and inhibit osteoclast bone resorption. However, the presence of wear debris can lead to an influx of inflammatory cytokines and chemokines and create an imbalance in the RANK/RANKL/OPG Pathway [13, 16, 17]. This imbalance leads to an increase in osteoclasts numbers and activity leading to bone resorption, osteolysis, and aseptic loosening of the implant.

Adverse Local Tissue Reactions

Adverse Local Tissue Reactions (ALTR) have been observed in TJA due to Mechanically Assisted Crevice Corrosion (MACC) [18]. Hall et al. defines ALTR as a "combination of aseptic masses, aseptic lymphocyte-dominated vasculitis-associated lesions (ALVALs), soft and hard tissue necrosis, and osteolysis in association with a joint replacement" [19]. Histopathology of ALTR in periprosthetic tissue features destruction of the synovial surface, inflammatory fibrin exudate (i.e. pus), and widespread necrosis [19]. In cases of ALTR caused by MACC, particles of corrosion products are often seen present in the tissues surrounded by giant cells. Diagnosis of ALTR is typically performed by analyzing the concentrations of metal ions in the blood. However, this method can be unreliable and does not provide a definitive prediction of periprosthetic tissue damage [20].

Toxicity of Metal Ions

Many of the constituents of metal alloys used in orthopaedic implants, such as cobalt, chromium, vanadium, and nickel, are naturally occurring as metal ions in the human body and required for normal homeostasis [12]. Normal human serum levels of these implantable metals are identified as Cr: 0.15 ng/mL, Co: 0.2 ng/mL, Al: 1-10 ng/mL, Ti: <4.1 ng/mL, and V: <0.01 ng/mL [11]. However, excessive levels of these trace metals have been linked to serious adverse medical conditions. Excessive amounts of Co have been linked to polycythemia, hypothyroidism, cardiomyopathy, and carcinogenesis. Excessive levels of Cr have been linked to nephropathy, hypersensitivity, and carcinogenesis. Excess Nickel has been linked to eczematous dermatitis, hypersensitivity, and carcinogenesis. And excess Vanadium has been linked to cardiac and renal dysfunction, hypertension, and manic-depressive psychosis [15, 21].

In a study by Houdek et al. investigating the significance of synovial fluid metal ion levels in predicting ALTR, patients with ALTR had synovial fluid Co and Cr levels 120 times higher than patients without ALTR and 414 times higher than Co and Cr levels in whole blood [20]. In a study by Plummer et al following 27 patients undergoing revision THA due to ALTR, mean blood serum levels were analyzed prior to and after revision surgery. Preoperative serum levels for cobalt were elevated in all patients, and cobalt serum levels were significantly greater than chromium serum levels (Co: 11.2 ppb and Cr: 2.2 ppb; $P<0.0001$). Sixteen of the 27 patients had their serum levels measured 2-4 years post-op. In each case, a decrease in both the serum cobalt (0.33 ppb; $P=0.004$) and chromium (0.51 ppb; $P=0.001$) levels was observed [22].

Inflammatory Cell-Induced Corrosion

Metal alloys, specifically CoCr and TiAlV, are frequently used in TKA and THA implants. In a retrieval study of hip and knee implants by Gilbert et al., a new form of corrosion was identified and termed "Inflammatory Cell-Induced Corrosion" (ICIC) [2]. Gilbert's group hypothesized that the observed ICIC damage was due to an immune response against the implant's wear debris and metal ions, leading inflammatory cells to directly attack the metal implant surface. Evidence of ICIC damage (**Figure 1-2**) was observed in damage patterns containing discolored regions with small cell-sized pits with circular and irregular crater-like features on the surface of retrieved TKA and THA implants [2]. The inflammatory cells thought to be engaging in this ICIC corrosion include osteoclasts, macrophages, foreign body giant cells and polymorphonuclear leucocytes [18]. These inflammatory cells are known to release Reactive Oxygen Species (ROS) including hydrogen peroxide (H_2O_2) and hypochlorous acid (HClO) [15]. Introduction of these ROS increases the corrosion susceptibility of certain metal alloys, specifically CoCrMo, by causing damage and degradation to the protective oxide layer [5].

Since the prevalence of ICIC is still uncertain, many groups have been investigating the incidence of ICIC in TJA implants retrieved from revision and necropsy [2, 6, 7, 23]. Gilbert et al. analyzed 69 different CoCrMo retrieved components from 51 implant systems including 18 hip liners, 37 heads, and 14 knees that were implanted for 0.1-17.9 years [2]. Of those implants, 51 different components (74%) displayed ICIC damage patterns [2]. In a retrieval study by Di Laura et al., 100 failed CoCr alloy hips with metal-on-metal (MOM) bearings were examined for signs of ICIC damage. Of Di Laura's implants, 59% possessed evidence of surface damage consistent with the signs of ICIC damage [7]. In a retrieval study by Arnholt et al., 52 femoral condyles that were implanted for at least 15 years were examined for incidence of MOM wear, MACC at taper interfaces, cement interface corrosion, third-body abrasive wear, and inflammatory cell-induced corrosion (ICIC) [23]. Of those 52 implants, 51 (98%) displayed surface damage indicative of corrosion and/or wear. While only 15 (29%) of the femoral components displayed damage consistent with ICIC patterns and saw a median cumulative ICIC damage area of 0.07 mm^2 [23]. However, the before-mentioned studies

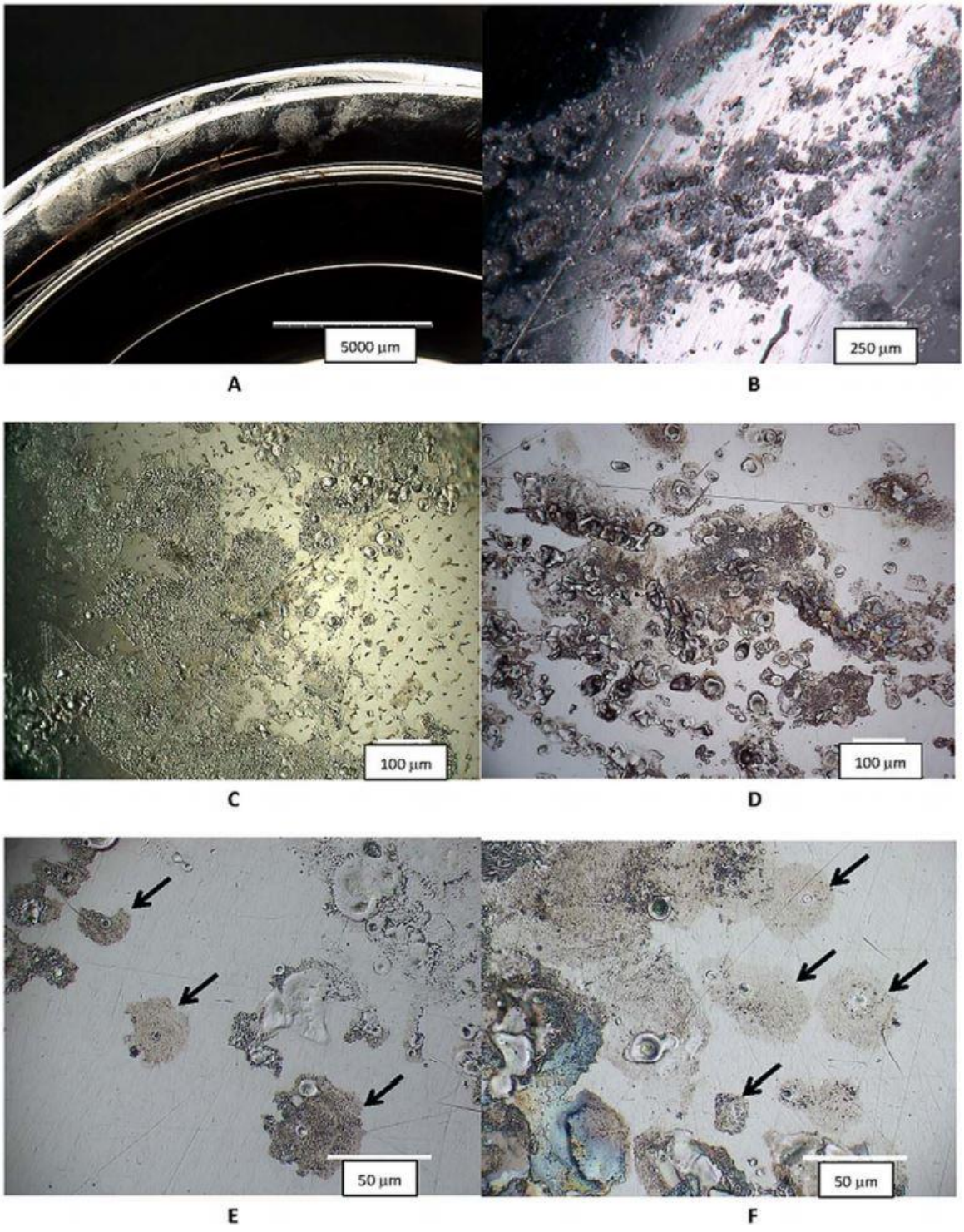

Figure 1-2. Digital Optical Micrographs of ICIC Damaged CoCr Hip Implants
Reprinted with permission. Gilbert, Jeremy L., et al. "Direct in vivo inflammatory cell-induced corrosion of CoCrMo alloy orthopedic implant surfaces." Journal of Biomedical Materials Research Part A 103.1 (2015):211-223 [2].

all examined implants retrieved from revision surgery. In a study by Heise et al. examining 41 CoCr TKA specimens retrieved from necropsy specimens, the incidence of ICIC damage was much lower [6]. Only 7 of the 41 implants (17%) displayed signs of damage indicative of ICIC [6]. This has led many to believe the reports from retrieval studies examining time-of-revision retrieved implants may be skewed and reporting evidence of both ICIC and EC damage.

Electrocautery Damage

Electrosurgery is the clinical application of high frequency alternating currents to living tissue [24]. The concept of electrosurgery dates back to 980 BC when Albucasis described using a hot iron to control bleeding in patients [25]. Primary applications of electrosurgery include cutting and coagulation. Electrosurgery devices include Electrocautery (EC) devices which are commonly used in many medical applications, including during TKA. There are two types of EC devices, Bipolar (BP) (**Figure 1-3**) and Monopolar (MP) (**Figure 1-4)**. BP EC devices, also known as an Aquamantys, utilize an electrode with two separate terminals, with one electrode producing the current and the other acting to bring the current back to the electrode. MP EC devices, also known as a Bovie, utilize an electrode with a single terminal that produces current and a dispersive electrode, separate from the system, to draw the current back to the surgical unit [24]. Electrosurgical units work by supplying a high frequency current, higher than 10 kHz, that is capable of passing through the body and generating heat due to the tissue's resistance [26, 27]. This heat generation is capable of coagulating blood vessels and cutting tissues by dissipating into the surrounding tissue. Due to the high current density needed to cut through tissue, an electrical arc can occur due to the voltage difference between the electrode and tissue [24]. This electrical arcing has been observed in TJA revision case studies and has been seen to cause damage to implant surfaces due to the close proximity of the EC device to the metal implant [28]. This EC arc damage includes melting, pitting, and oxide formation on the metal alloy surface.

The similarities in the damage patterns occurring between EC damage and ICIC corrosion patterns has led to the development of two trains of thought. The first being that damage patterns being observed are due to inflammatory cells altering the implant oxide layer, and the second being that the damage patterns being discovered are actually from surgeons using an EC device close to the implant surface. These trains of thought have led multiple labs to look into the similarities and differences between ICIC and ECIC damage patterns. Yuan et al. examined 1859 retrieved metal implants to examine the presence of pitting and crater-like features similar to ICIC and ECIC damage patterns. Yuan et al. also induced EC damage on a polished CoCr surface using a standard Bovie tip at 70 volts and used methods "mimicking" surgical methods such as dotting the Bovie tip, dragging the Bovie tip, and hovering the Bovie tip [12]. In a retrieval study performed by Gilbert et al. composed of 69 components, saw that 74% of components possessed the unique corrosion patterns believed to be due to ICIC. Kubacki et al. investigated if electrosurgical units were capable of reproducing damage patterns similar

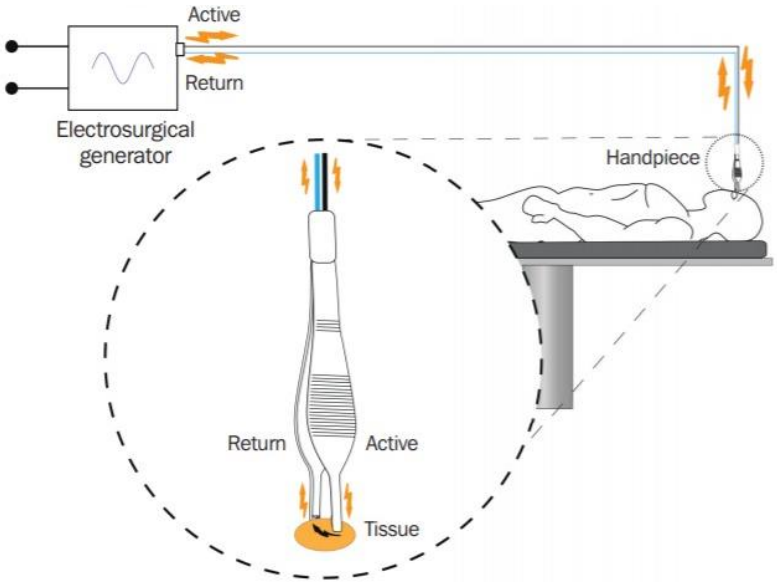

Figure 1-3. Principle of Bipolar Electrosurgery
The surgical effect arises due to tissue heating caused by the current flow between the two closely spaced electrodes.
Reprinted with open access permission. Ismael Cordero. "Electrosurgical Units – How They Work and How to Use Them Safely." Community Eye Health Journal, vol. 28, no. 89, June 2015, pp. 15–16. [29]

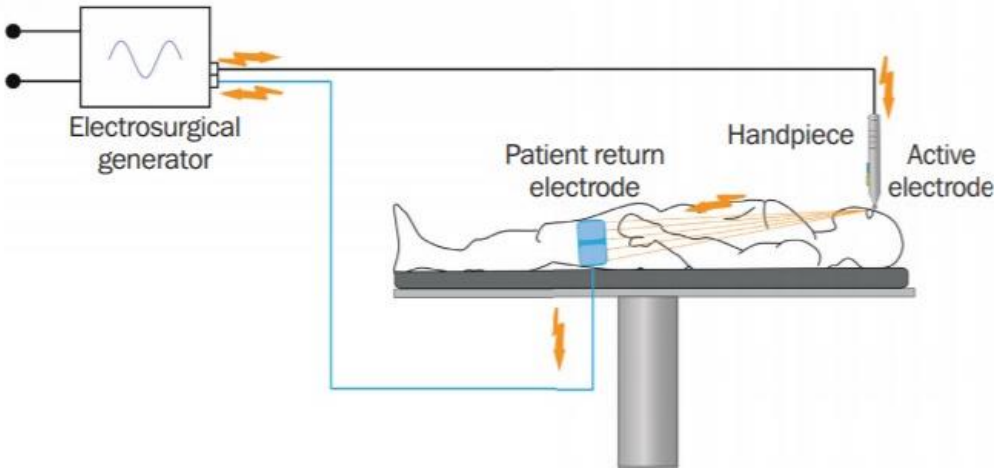

Figure 1-4. Principle of Monopolar Electrosurgery
The surgical effect arises due to tissue heating caused by the current flow at the active electrode where the current density is highest.
Reprinted with open access permission. Ismael Cordero. "Electrosurgical Units – How They Work and How to Use Them Safely." Community Eye Health Journal, vol. 28, no. 89, June 2015, pp. 15–16. [29]

to the corrosion patterns believed to be ICIC. CoCr and Ti6Al4V disks were polished and then introduced to an EC device with dry contact, wet contact, 1 mm thick agarose hydrogel, and 3 mm thick agarose hydrogel. Both materials and experimental groups displayed EC damage patterns similar to ICIC corrosion patterns [28]. Heise et al. analyzed the chemical profile of 41 implants retrieved postmortem and identified 7 implants (17%) possessing signs of ICIC damage. Heise et al. also intentionally damaged 3 different implant bearing surfaces with a MP and BP EC device at varying power levels and saw that the areas damaged by EC had a higher Fe/C ratio than those damaged areas believed to be ICIC. Discrepancies in the occurrence of ICIC damage (17% or 59%) from retrieval studies solidifies the debate on whether the damage patterns being observed are from ICIC or careless surgeons eliciting ECIC.

Objectives and Hypothesis

With the number of primary TKAs increasing yearly due to increased population size, obesity rates, and better access to healthcare, the need to understand the cause of these damage mechanisms and their biological responses is paramount. With increased TKA procedures, the rate of revision surgeries is expected to increase if the complications arising from these TKA implants are not addressed. Understanding the biological responses and characteristics of TKA implants with and without existing oxide layer damage will provide insight into the clinical significance of damage patterns previously seen from retrieval studies. To better understand how EC alters an implant surface, three different types of TKA bearing surfaces were intentionally damaged with both a MP and BP EC device at varying power levels. Our first objective was to identify how the surface roughness parameters differed between EC device, power, and bearing surface type using a surface profilometer. Our second objective was to examine the damaged and undamaged areas for each bearing type under SEM and detect any elemental differences between the two damage mechanisms. We hope to determine the significance of this damage mechanism and identify its characteristics. To better understand the effect of macrophages on the surface of CoCr alloy, IC-21 macrophages were allowed to adhere to the surface of metal disks for 30-days and activated using LPS and IFNγ. Some disks also experienced oxide layer damage by being intentionally damaged using a MP EC device to identify any differences in biological response. For these studies, the following experimental hypotheses were tested.

a) There will be a difference in the roughness parameters of the areas damaged with a MP or BP EC device compared to undamaged implant surface areas.

b) There will be a difference in the elemental makeup of the MP and BP damaged surfaces compared to undamaged surface areas.

c) Macrophages cultured on CoCr disks are capable of ingesting metal ions from the surface of the CoCr disks and will be capable of affecting the surface with a pitting damage to the oxide surface layer.

d) Macrophages cultured on CoCr disks damaged with an EC device will display higher intracellular metal ion concentrations compared to undamaged CoCr disks. The supernatant fluid from EC damaged Disks will have a higher metal ion concentration.

CHAPTER 2. ELECTROCAUTERY INDUCED DAMAGE OF TOTAL KNEE IMPLANTS[1]

Background

Total Knee Arthroplasty (TKA) is commonly performed for treatment of osteoarthritis and rheumatoid arthritis. However, of patients that undergo TKA, about 10-15% of patients still report unsatisfactory results compared to their expectations and 30% of patients report long-term pain and/or some kind of functional deficit [30-32]. Common causes of implant failure include periprosthetic joint infection, instability, periprosthetic fracture, arthrofibrosis, polyethylene wear, suboptimal alignment of the implant, and extensor mechanism deficiency [4].

Evidence of direct pitting on the surface of CoCrMo alloy implants for both hip and knee implants has been seen in several retrieval studies [2, 12, 28]. However, the mechanism leading to this pitting has been controversial and has many researchers disputing the following hypothesis. The first hypothesis, recently put out as a new form of corrosion termed Inflammatory Cell-Induced Corrosion (ICIC), observed by Gilbert et al., was identified by frosted regions with circular or irregular shaped crevices and pits [2]. Gilbert's group hypothesizes that the metal ions and wear particles brought about due to MACC ensures an immune response in some patients. This immune response leading to the direct attack of inflammatory cells on the surface of metal implants. However, a different hypothesis reported by Gilbert and Campbell suggests that the damage patterns observed are caused by the plasma arc coming off the EC tools when in close proximity to the metal implant during primary implant removal during revision. Recent studies have shown that the use of EC can damage the passive oxide layers of implants [30-32].

The goal of this study was to compare the surface profile of different implant bearing surfaces that underwent intentional EC damage using a MP device and a BP device. We believed that the surface roughness parameters of the areas damaged by EC devices would be greater than areas not damaged by EC devices. Between implant types, we believed that ceramic surfaces would be less vulnerable to EC damage mainly due to the insulating properties ceramics have from an EC produced plasma arc and that the CoCr would have the greatest surface damage since it is an electrical conductor. Looking at the surface chemical profiles for each bearing type and EC damage type, we believed there would be differences in the surface chemical profile between MP and BP damaged areas and between undamaged areas.

---

[1] Modified from final submission with permission. Miller KC, Morrow BR, Sorrels JH, Arnholt CM, Mihalko WM. Electrocautery Induced Damage of Total Knee Implants. *The Journal of Arthroplasty*. 2021;36(3):1126-1132. doi: https://doi.org/10.1016/j.arth.2020.09.044

Materials and Methods

Electrocautery Damaged Specimens

For this study, three different types of femoral component bearing surfaces were selected including a CoCrMo alloy bearing surface (Aesculap Inc), a multilayer zirconium nitride (ZrN) bearing surface (Aesculap Inc), and Oxinium bearing surface (Smith & Nephew Inc). The 3 implants were all taken into the operating room and intentionally damaged using the plasma arc from both MP (Bovie) and BP (Aquamantys) sources **(Figure 2-1)** using a three-second hover method. Damage for the MP EC device was done at 30W, 45W, and 60W. BP EC device damage was done at 140W, 180W, and 220W. In order to remove any loose debris from the EC damage, the implants were soaked in separate solutions of water and detergent at a ratio of 10:1 for two consecutive 20-minute rounds and rinsed with cold deionized water between soaks. Implants were then ultrasonicated in a bath of deionized water with a few drops of detergent for two consecutive 30-minute increments. Finally, implants were rinsed off in cold deionized water and set to dry overnight under a fume hood.

Surface Topography

A profilometer (DektakXT; Bruker, Tucson, AZ) with a 2.5-µm radius stylus was used to assess an area of 3.8 mm by 3.2 mm in the central portion of the damaged area for each MP and BP energy setting for each implant. The damaged areas were evaluated with the aid of TalyMap (Mountains software; Digital Surf, Bescançon, France) using ISO 4287 measurements for R_a (arithmetic average height parameter), R_z (maximal distance between highest peak and lowest valley), R_k (kurtosis), and R_{sk} (skewness) (**Figure 2-2**). With R_a being the most universally used measure of the roughness parameter for general quality control. R_z representing the measure of maximum distance between the highest peak and lowest valley. R_k representing the measure of how abruptly the surface topography changes over an area. R_{sk} representing the variability of the changes of the surface over a given area.

Scanning Electron Microscopy and Electron Dispersion X-Ray Spectroscopy

Scanning electron microscopy (SEM) (Ziess, Oberkochen, Germany) was used to obtain a detailed microscopic analysis of the areas damaged by EC. SEM imaging was performed at 20 kV for initial damage assessment of the implants. Energy-dispersive X-ray spectrometry (EDS) (Oxford, High Wycombe, UK) was used to assess the presence of elements in the pits found in corroded areas by focusing the electron beam and capturing the characteristics of the X-rays emanating from the implant surface.

Figure 2-1. Damaged Areas Shown on ZrN-, CoCr-, and Oxinium-Bearing Surfaces
Left to Right: ZrN-Bearing Surface, CoCr-Bearing Surface, and Oxinium-Bearing Surface

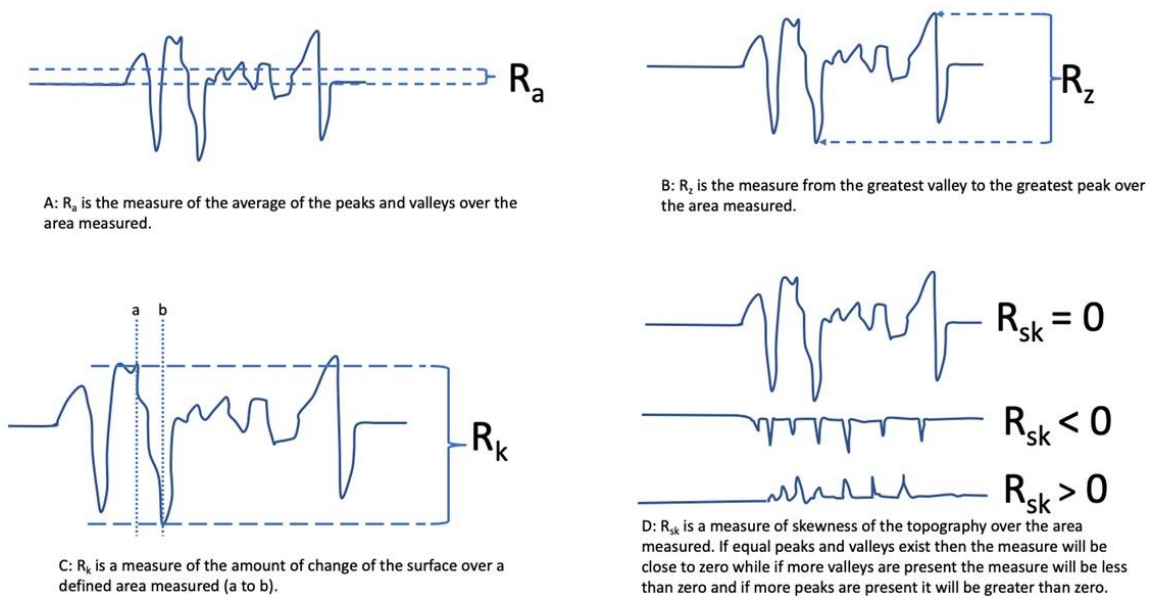

A: R_a is the measure of the average of the peaks and valleys over the area measured.

B: R_z is the measure from the greatest valley to the greatest peak over the area measured.

C: R_k is a measure of the amount of change of the surface over a defined area measured (a to b).

D: R_{sk} is a measure of skewness of the topography over the area measured. If equal peaks and valleys exist then the measure will be close to zero while if more valleys are present the measure will be less than zero and if more peaks are present it will be greater than zero.

Figure 2-2. ISO 4287 Roughness Parameters

Statistical Analysis

All data was tested for normality and equal variance before any statistical analyses were performed. Shapiro-Wilk normality tests were performed using Microsoft Excel (Microsoft, Redmond, WA) and revealed that the surface topography and EDS data sets were not normally distributed. MP (Bovie) and BP (Aquamantys) sources at the various energy levels were combined for each of the bearing surfaces and compared. A Kruskal-Wallis test and post hoc Dunn's multiple comparison test were used for comparing the R_a, R_z, R_k, and R_{sk} roughness parameters among the EC-damaged areas with the nondamaged areas of the implants using SigmaPlot (Systat Software, Chicago, IL). Comparisons were made for the EDS analysis for the EC-damaged areas of the implants with the nondamaged areas of the implants using Mann-Whitney rank sum tests in SigmaPlot (Systat Software, Chicago, IL).

Results

Surface Topography

Mean roughness measurements obtained from the surface profilometry are listed in **Table 2-1.** The Oxinium-bearing surface displayed the highest mean valley-to-peak R_z roughness measurements for both the MP and BP compared to the other bearing surface. With the ZrN-bearing surface displaying the lowest R_z measurements. The R_a roughness parameter for the Oxinium surface displayed the greatest difference of all 3 bearing surfaces for the MP device. For skewness (R_{sk}), the CoCr surface displayed the greatest skewness for the BP damaged areas. The R_k values for all 3 bearing surfaces were very similar for the MP damaged areas, and the Oxinium showed the greatest change in R_k for the BP damaged areas.

Comparing the MP damage to an undamaged area on the Oxinium implant showed a significant difference for R_z and R_a ($P=0.04$). The CoCr-bearing surface only saw significant differences in the R_{sk} parameter when compared between the BP area and an undamaged area ($P=0.04$). The ZrN-bearing surface saw significant differences when the MP R_z and BP R_{sk} were compared to an undamaged area ($P=0.04$ for both R_z and R_{sk}). While the changes seen for the BP damage in all bearings, the Oxinium implant showed the largest values and changes in R_z and R_a measurements for both MP and BP damage compared to an undamaged area. The ZrN had the smallest differences in R_z and R_a for both MP and BP damage areas compared to undamaged areas.

SEM and EDS

The EDS Backscatter Analysis for the 3 bearing surfaces can be seen in **Tables 2-2** through **2-4**. For the CoCr-bearing surface, there was significantly more Cr and Co measured using the MP device compared to the BP at all energy levels ($P<0.01$). When

Table 2-1. Mean ISO 4287 Profilometric Measurements of R_a, R_z, R_{sk}, R_k for the Oxinium-, CoCr-, and ZrN-Bearing Surfaces

Group		R_z (µm)	R_a (µm)	R_{sk} (µm)	R_k (µm)
Oxinium	MP Damaged Areas	1.800	0.317	0.387	2.980
	BP Damaged Areas	0.512	0.081	0.077	3.010
	Undamaged Areas	0.372	0.093	0.076	2.040
CoCr	MP Damaged Areas	0.510	0.093	0.653	3.177
	BP Damaged Areas	0.455	0.087	0.311	2.410
	Undamaged Areas	0.464	0.076	-0.479	2.950
ZrNt	MP Damaged Areas	0.378	0.058	-0.007	3.090
	BP Damaged Areas	0.397	0.068	0.069	2.607
	Undamaged Areas	0.273	0.057	-0.162	2.120

Table 2-2. Backscatter Nonparametric Statistical Analysis for the Oxinium-Bearing Surface

Background Element	Electrocautery Comparison	Mean Rank Difference	Adjusted P Value
Carbon	BP vs Undamaged	26.2	0.001*
	MP vs Undamaged	13.3	0.234
	MP vs BP	12.9	0.044*
Sodium	BP vs Undamaged	29.3	<0.001*
	MP vs Undamaged	28.5	<0.001*
	MP vs BP	0.8	1
Aluminum	BP vs Undamaged	10.7	0.01*
	MP vs Undamaged	2.3	1
	MP vs BP	12.9	0.002*
Titanium	BP vs Undamaged	12.6	0.05*
	MP vs Undamaged	27.2	<0.001*
	MP vs BP	14.6	0.003*
Chromium	BP vs Undamaged	9.2	0.486
	MP vs Undamaged	18.1	<0.001*
	MP vs BP	8.9	0.436
Iron	BP vs Undamaged	11.2	0.172
	MP vs Undamaged	23.2	<0.001*
	MP vs BP	12.0	0.059

Oxinium-bearing surface energy dispersive x-ray spectroscopy analysis Kruskal-Wallis one-way analysis of variance on ranks.
*indicates statistical significance for the comparison listed

Table 2-3. Backscatter Nonparametric Statistical Analysis for the Cobalt Chrome-Bearing Surface

Background Element	Electrocautery Comparison	Mean Rank Difference	Adjusted P Value
Carbon	BP vs Undamaged	43.3	<0.001*
	MP vs Undamaged	36.4	<0.001*
	MP vs BP	6.9	0.695
Magnesium	BP vs Undamaged	22.1	0.025*
	MP vs Undamaged	18.6	0.101
	MP vs BP	3.4	1
Chromium	BP vs Undamaged	35.0	<0.001*
	MP vs Undamaged	21.7	0.04*
	MP vs BP	13.3	0.062
Iron	BP vs Undamaged	21.6	<0.001*
	MP vs Undamaged	17.5	<0.001*
	MP vs BP	4.0	1
Cobalt	BP vs Undamaged	35.3	<0.001*
	MP vs Undamaged	35.9	<0.001*
	MP vs BP	0.5	1
Nickel	BP vs Undamaged	8.9	0.007*
	MP vs Undamaged	9.2	0.027*
	MP vs BP	0.3	1
Molybdenum	BP vs Undamaged	19.8	0.017*
	MP vs Undamaged	18.7	0.069*
	MP vs BP	1.1	1

Cobalt Chromium-bearing surface energy dispersive x-ray spectroscopy analysis
Kruskal-Wallis one-way analysis of variance on ranks.
*indicates statistical significance for the comparison listed

Table 2-4. Backscatter Nonparametric Statistical Analysis for the Zirconium Nitride-Bearing Surface

Background Element	Electrocautery Comparison	Mean Rank Difference	Adjusted P Value
Carbon	BP vs Undamaged	39.8	<0.001*
	MP vs Undamaged	29.0	<0.001*
	MP vs BP	10.8	0.165
Nitrogen	BP vs Undamaged	1.5	1
	MP vs Undamaged	18.2	0.006*
	MP vs BP	16.7	<0.001*
Sodium	BP vs Undamaged	28.8	0.012*
	MP vs Undamaged	35.8	<0.001*
	MP vs BP	7.0	0.741
Chromium	BP vs Undamaged	28.0	0.016*
	MP vs Undamaged	50.8	<0.001*
	MP vs BP	22.9	<0.001*
Iron	BP vs Undamaged	19.5	<0.001*
	MP vs Undamaged	21.5	<0.001*
	MP vs BP	1.9	1
Cobalt	BP vs Undamaged	3.8	1
	MP vs Undamaged	20.3	<0.001*
	MP vs BP	16.5	0.046*
Zirconium	BP vs Undamaged	22.0	<0.001*
	MP vs Undamaged	54.0	<0.001*
	MP vs BP	32.0	0.004*

Zirconium Nitride-bearing surface energy dispersive x-ray spectroscopy analysis
Kruskal-Wallis one-way analysis of variance on ranks.
*indicates statistical significance for the comparison listed

comparing MP to BP on the Oxinium surface damaged areas, there were significant differences in carbon, aluminum, and titanium (P = 0.04, 0.002, and 0.003 respectively). Comparing the MP to BP damaged areas on the ZrN-bearing surface, there were significant differences in nitrogen, chromium, cobalt, and zirconium (all P < 0.001) with the MP areas being greater than the BP Areas.

Visual assessment (**Figures 2-3** through **2-5**) of the MP damaged areas showed a darkened area on the surface of the CoCr- and ZrN-bearing surfaces. However, the black color of the Oxinium made the damage unnoticeable. The damaged areas visually seen on the CoCr- and ZrN-bearing surfaces ranged in size from 2-3 mm in width to 4-5 mm in length. EC damaged areas under the SEM consisted of discolored regions with pitting and crater-like features, consistent with reports from previous retrieval studies [7, 12].

Discussion

The use of a BP (Aquamantys) vs an MP (Bovie) in this in vitro study found that the BP imparted less damage on all 3 surfaces by topography measures as well as subjective comparisons. The ZrN showed the least damage of the 3 surfaces, as determined by R_z and R_a values, while the Oxinium-bearing surface saw the largest changes. Our SEM and topography findings support previous observations of corrosion evidence occurring on knee implants [7, 23, 30, 32].

To understand the topography changes on the surface due to the 2 damage mechanisms, R_a, R_z, R_{sk}, and R_k roughness parameters were calculated. In a study by Heyse et al.[33], the mean (± standard deviation) roughness parameters of pristine CoCrMo knee implants were observed as R_a = 0.04 µm (±0.003), R_z = 0.636 µm (±0.042), and R_{sk} = 0.33 µm (±1.17). The roughness values from our study were in a similar range. The slightly higher roughness values we determined in undamaged areas most likely resulted from damage from shipping the implants between our 2 collaborating research laboratories. For all 3 implant surfaces, both MP and BP EC damaged areas displayed an increase in R_z and R_a roughness parameters compared to nondamaged areas. Previous studies have shown that an increase in roughness values indicated more implant damage and possible debris on the implant surface, possibly resulting in more polyethylene wear. The increase in the roughness parameters measured could be due to the pitting seen in other time-of-revision implant retrieval analyses. Results from the elemental backscatter SEM analysis further emphasized the greater damage imparted by the MP and BP EC devices. The EDS portion of the study verified that the MP device seemed to uncover more substrate material for all 3 surfaces. It also appeared that there was not significant transfer of material from the EC tip to the implant surface. However, this material transfer could have been removed during the cleaning process.

Limitations to this study include the in vitro nature of our EC-induced damage. While the SEM images display similarities to those reported in time-of-revision retrieval studies, there could still be differences in the local environment that could impart

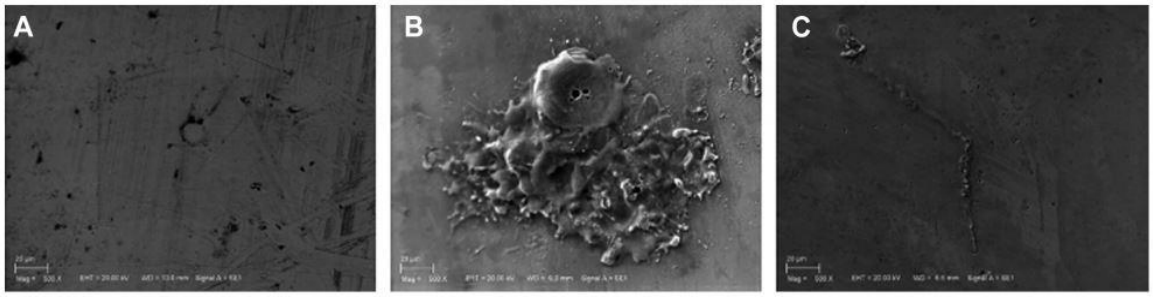

Figure 2-3. SEM Images for the CoCr-Bearing Surface
(A) Undamaged, (B) MP (60W) and (C) BP (180W)

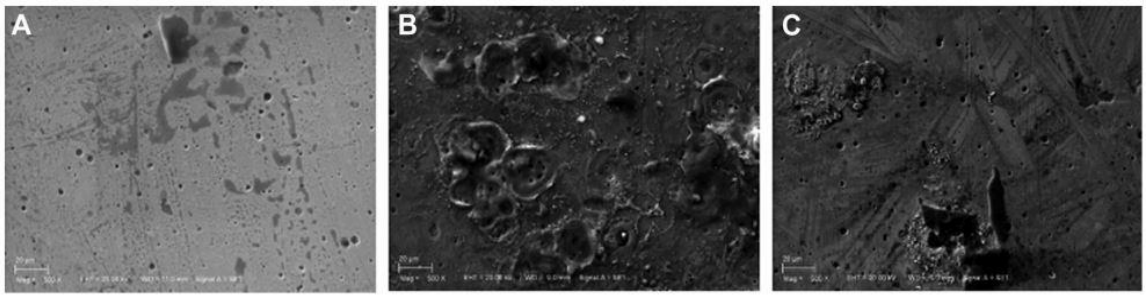

Figure 2-4. SEM Images for the Zirconium Nitride-Bearing Surface
(A) Undamaged, (B) MP (60W) and (C) BP (180W)

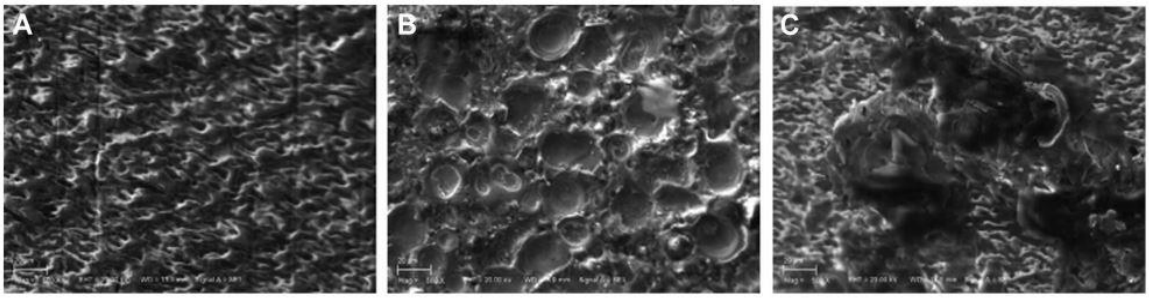

Figure 2-5. SEM Images for the Oxinium-Bearing Surface
(A) Undamaged, (B) MP (60W) and (C) BP (180W)

differences that may result in less harsh damage than those modeled in this study [7, 23, 30, 32]. The clinical significance of our findings is still uncertain and the need for further study on the possible effects of wear and metal ion release persists.

CHAPTER 3. IN VITRO EFFECTS OF MACROPHAGES ON COCR ALLOYS WITH AND WITHOUT ELECTROCAUTERY DAMAGE

Background

Orthopaedic implants have utilized certain metal alloys for a variety of applications due to their high mechanical strength and relatively good biocompatibility. However, these metal alloys are not completely inert and still experience a variety of corrosion mechanisms which may lead to complications in the local tissue environment including adverse local tissue reactions. These ALTR include pseudotumors, ALVAL, metallosis, and necrosis. It is believed these ALTR are brought about due to the activation and attack of inflammatory cells such as macrophages. Local inflammatory response from macrophages, and other phagocytic inflammatory cells, create a harsh environment of ROS (including H_2O_2, HClO, superoxide and hydroxyl radicals) [5]. The release of ROS into the environment disrupts the reformation of the passive oxide layer, increasing the corrosion susceptibility of CoCrMo alloy. It is believed that these macrophages, while supplying inflammatory cytokines in the local environment, are also directly attacking the implant surface and ingesting metal particles.

Several retrieval studies [2, 7, 23] have observed TKA implant damage patterns believed to be due to inflammatory cell-induced corrosion. However, many of these studies looked at TJA components retrieved from time of revision which could lead to misinterpretations in the occurrence of ICIC. In a retrieval study looking only at necropsy specimens by Heise et al., the incidence of ICIC damage was lower (17%) than incidence described in the literature (59%). Discrepancies in the cause of these damage areas has led to two viewpoints on the damage mechanism: (1) that Inflammatory cells are attacking and damaging the oxide layer of these metal alloys, or (2) that the damage is due to surgeons using EC devices near the implant surface during surgery. Many studies have attempted to simulate the synovia environment, but many fail to also include a biological aspect like macrophages into their studies. In another study by Heise et al., the possibility of macrophages affecting the oxide layers of orthopaedic alloys was investigated and evidence was found suggesting that these cells can affect the oxide layer and release metal ions into the surrounding local tissue environment [34]. However, a limitation of this study was that it did not pursue investigation into the phagocytic ability of macrophages ingesting metal particles or the effects of existing damage to the metal oxide layer.

The goal of this study is to examine the mechanisms of cellular corrosion by examining if macrophages on the surface of orthopaedic grade CoCr metal can damage the surface oxide layer and if metal ions can be found inside the cells. IC-21 murine peritoneal macrophages were cultured on ASTM F1537 CoCr disks with and without EC damage to stimulate existing oxide layer damage. As well as, with and without proinflammatory activators to stimulate local inflammatory response in the human body. It is hypothesized that both activated and non-activated cells will be able to degrade and

change the surface oxide layer of the alloys by ingesting metal particles and that the cells will release metal particles into their environment [35].

Materials and Methods

Disk Preparation

ASTM F1537 Cobalt Chrome bar stock with a diameter of 0.25 inches was purchased from M. Vincent & Associates (Minneapolis, MN) and then cut into disks with varying thicknesses at the University of Memphis machine shop. The disks were then polished to a mirror finish using an EXAKT 400Cs Micro Grinding System with 320, 500, 800, 1000, 1200, and 2000 abrasive grit paper. After polishing, disks were cleaned by sonication with warm alkaline detergent, rinsed with deionized water and passivated in 30% nitric acid to restore the oxide layer. They were then rinsed with deionized water again and placed in an ultrasonicator for two 30-minute increments, rinsing the disks in between each increment. The disks were then sterilized under the UV lamp in the culture hood for 12 hours.

A repeat of the experiment included the same F1537 Cobalt Chrome bar stock with a diameter of 0.25 inches purchased from M. Vincent & Associates (Minneapolis, MN) and then cut into disks with varying thicknesses at the University of Memphis machine shop. During this repeat, the disks were polished to a mirror finish using an EXAKT 400CS Micro Grinding System with 320, 500, 800, 1000, 1200, 2000, and 4000 abrasive grit paper. The same cleaning process as before was used for these disks.

Several CoCr disks were later taken into the operating room at Methodist University Hospital (Memphis, TN) and damaged with the plasma arc from a Bovie electrocautery device using a three-second hover method at 45W 3mm from the disk surface.

Macrophage Preparation

IC-21 (ATCC TIB-186, American Type Culture Collection, Manassas, VA) peritoneal mouse macrophages were cultured to a concentration of 600×10^3 cells/mL. The macrophages were cultured in a growth medium of RPMI 1640 with 10% Fetal Bovine Serum (Sigma), 1% L-glutamine (Sigma), and 0.13% gentamicin (Sigma). Macrophages were grown in 75 cm^2 flasks and cultured in a humidified incubator at 37°C with 5% CO_2. Growth Medium was changed every 2 to 3 days.

Experimental Conditions

ASTM 1537 CoCr disks were placed into 96 well plates where cells were then added and allowed to adhere for 24 hours. An endogenous activator, Interferon Gamma (IFNγ), and an exogenous activator, Lipopolysaccharide (LPS), were added to cell growth medium to induce macrophage activation. This led to eight experimental groups: (1) Undamaged Disks + Medium, (2) EC Damaged Disks + Medium, (3) No Disks + Medium, (4) Undamaged Disks + 20 x 10^3 cells/150 µL, (5) No Disks + 20 x 10^3 cells/150 µL, (6) Undamaged Disks + 20 x 10^3 cells/150 µL + 20ng/mL LPS + 20ng/ml IFNγ, (7) EC Damaged Disks +20 x 10^3 cells/150 µL + 20ng/mL LPS + 20ng/ml IFNγ, and (8) No Disks + 20 x10^3 cells/150 µL + 20ng/mL LPS + 20ng/ml IFNγ. Starting on Day 2, the culture medium was changed every 12 hours and the supernatant fluid was collected and frozen every 4 days for future analysis. Following 30 days, the cells were removed from the disk surface using two 150 µL/well washes of PBS. Cells were then digested using 1% Triton X100 and PBS. Disks were first soaked in a bath of water and detergent at a ratio of 10:1 for two consecutive 20-minute increments. Disks were ultrasonicated for two 30-minute periods in a water bath with diluted detergent.

A repeat of the experiment included the following groups: (1) Undamaged Disks + Medium, (2) EC Damaged Disks + Medium, (3) No Disks + Medium, (4) Undamaged Disks + 20 x 10^3 cells/150 µL, (4) EC Damaged Disks + 20 x 10^3 cells/150 µL, (6) No Disks + 20 x 10^3 cells/150 µL, (7) Undamaged Disks + 20 x 10^3 cells/150 µL + 20ng/mL LPS + 20ng/ml IFNγ, (8) EC Damaged Disks +20 x 10^3 cells/150 µL + 20ng/mL LPS + 20ng/ml IFNγ, and (9) No Disks + 20 x10^3 cells/150 µL + 20ng/mL LPS + 20ng/ml IFNγ. Cell Culture medium was still changed every 12 hours after the first day and supernatant fluid was collected and frozen every 4 days starting on day 2 for future analysis.

Metal Content Analysis

Collected supernatant fluid and digested cells were analyzed for trace metals using inductively coupled plasma triple quadrupole mass spectrometry (ICP-QQQ-MS) at Brooks Applied Labs (Bothwell, WA). The supernatant fluid and digested cells were tested for trace cobalt (Co), chromium (Cr), and molybdenum (Mo).

Scanning Electron Microscopy and Electron Dispersion X-Ray Spectroscopy

Scanning electron microscopy (SEM) (Ziess, Oberkochen, Germany) was used to obtain a detailed microscopic analysis of the CoCr disk surfaces after the experiment concluded. SEM imaging was performed at 20 kV for visual assessment of the disk surfaces to assess if the macrophages were able to alter the surface of the metal disks. Energy-dispersive X-ray spectrometry (EDS) (Oxford, High Wycombe, UK) was used to assess the elements present on the surface of the disks, and in pits found on the disk

surface, by focusing the electron beam onto the areas and capturing the characteristics of the X-rays reflecting off the surface.

Statistical Analysis

All data were tested for normality using a Shaprio-Wilk Test and for equal variance using a Brown-Forsythe Test before any statistical analyses were performed using Microsoft Excel (Microsoft, Redmond, WA). A Kruskal-Wallis One Way Analysis of Variance on Ranks with a post hoc Tukey test was utilized to compare the metal concentration of the supernatant fluid. This non-parametric test was used due to non-normal data and un-equal variance. All statistical tests were performed in SigmaPlot (Systat Software, Chicago, IL) with an assumed significance of $\alpha=0.05$.

Results

Metal Content

Cellular corrosion of the CoCr disks was quantified by measuring the concentration of Co, Cr, and Mo in the supernatant fluid collected off of the culture over the course of the 30-day experiment (**Figure 3-1**). Median Supernatant Fluid Metal Concentration can be seen in **Table 3-1**. Significantly elevated Co concentrations were found in the supernatant when comparing the Undamaged Disks with Activated Cells versus its control which contained medium with no cells ($P=0.004$). There was also a significantly higher Cr concentration in the supernatant fluid of the EC Damaged Disks with Standard Cells versus its control which contained medium with no cells ($P=0.005$).

Comparing the experimental groups against each other (**Table 3-2**), a significantly higher supernatant concentration of Co and Mo was seen in Undamaged Disks with Standard Cells compared to the EC Damaged Disks with Standard Cells. There was also a significantly higher Co concentration in the supernatant of the Undamaged Disks with Activated Cells compared to the EC Damaged Disks with Activated Cells. The EC Damaged Disks with Standard Cells also displayed a significantly less Cr concentration in the supernatant fluid compared to the EC Damaged Disks with Activated Cells.

The number of cells were counted following the end of the 30-day experiment (**Figure 3-2**). A statistically significant difference was seen between all cell groups ($P<0.001$) except when comparing the Undamaged Disks with Activated Cells versus the EC Damaged Disks with Activated Cells.

Following the end of the 30-day experiment, cells were digested to determine their inner metal ion concentration. The Co, Cr, and Mo intracellular concentration of the digested cells on Day 30 per 1000 cells can be seen in **Figure 3-3**. There was a

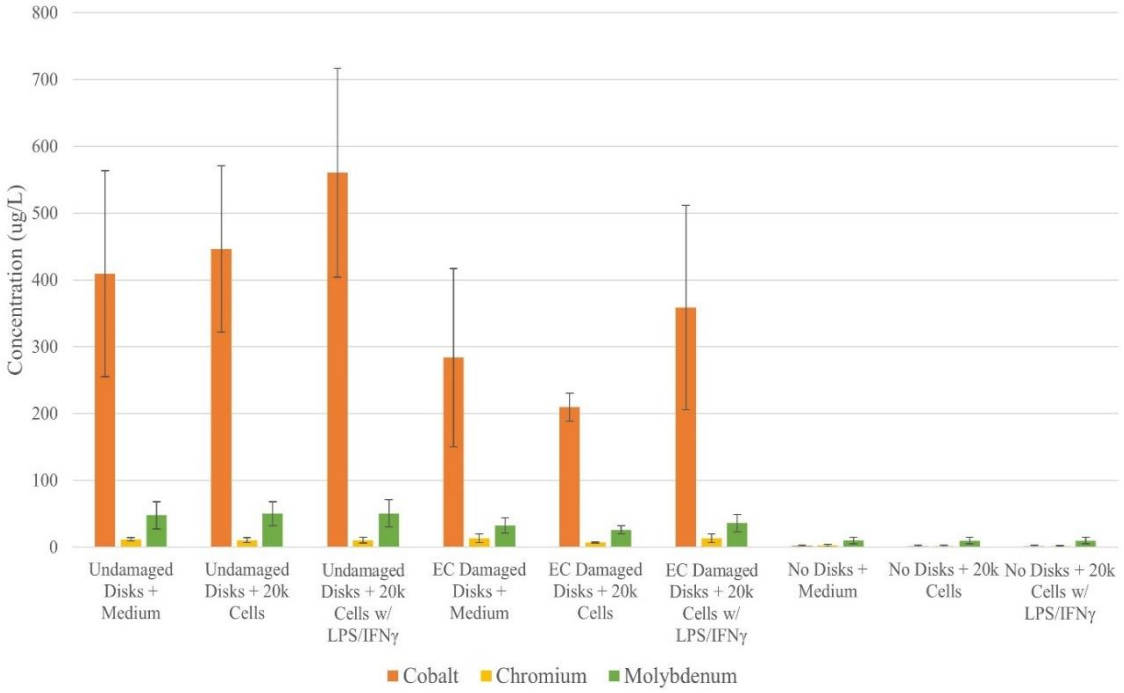

Figure 3-1. Supernatant Fluid Metal Concentration
Error bars represent ± one standard deviation

Table 3-1. Mean Supernatant Fluid Metal Ion Concentrations

Experimental Groups	Cobalt (ug/L)	Chromium (ug/L)	Molybdenum (ug/L)
Undamaged Disks + No Cells with Standard Medium	409±154	12±2	48±20
EC Damaged Disks + No Cells with Standard Medium	284±134	13±7	32±11
No Disks + No Cells with Standard Medium	1.9±1.2	2.5±1.7	10±5
Undamaged Disks + 20k Cells with Standard Medium	447±124	10±4	50±18
Undamaged Disks + 20k Cells with LPS/IFNy Medium	561±156*	10±4	51±20
EC Damaged Disks + 20k Cells with Standard Medium	209±21	7±0.9*	26±6
EC Damaged Disks + 20k Cells with LPS/IFNy Medium	359±153	13±6	36±13
No Disks + 20k Cells with Standard Medium	1.8±1.2	1.8±1	9.8±5
No Disks + 20k Cells with LPS/IFNy Medium	1.7±1.2	1.7±1	9.8±5

Statistical testing was performed to compare each experimental group with its control containing medium with no cells. *indicates $p<0.05$

Table 3-2. P-Values of the Pairwise Comparison of the Supernatant Fluid Metal Concentrations Between Experimental Groups

Group Comparison	Cobalt P Value	Chromium P Value	Molybdenum P Value
Undamaged Disks + 20k Cells with Standard Medium vs. Undamaged Disks + 20k Cells with LPS/IFNy Medium	0.091	1	0.163
Undamaged Disks + 20k Cells with Standard Medium vs. EC Damaged Disks + 20k Cells with Standard Medium	<0.001*	0.541	0.001*
Undamaged Disks + 20k Cells with LPS/IFNy vs. EC Damaged Disks + 20k Cells with LPS/IFNy Medium	<0.001*	0.617	0.056
EC Damaged Disks + 20k Cells with Standard Medium vs. EC Damaged Disks + 20k Cells with LPS/IFNy Medium	0.051	0.013*	0.731

*Indicates as statistically significant difference

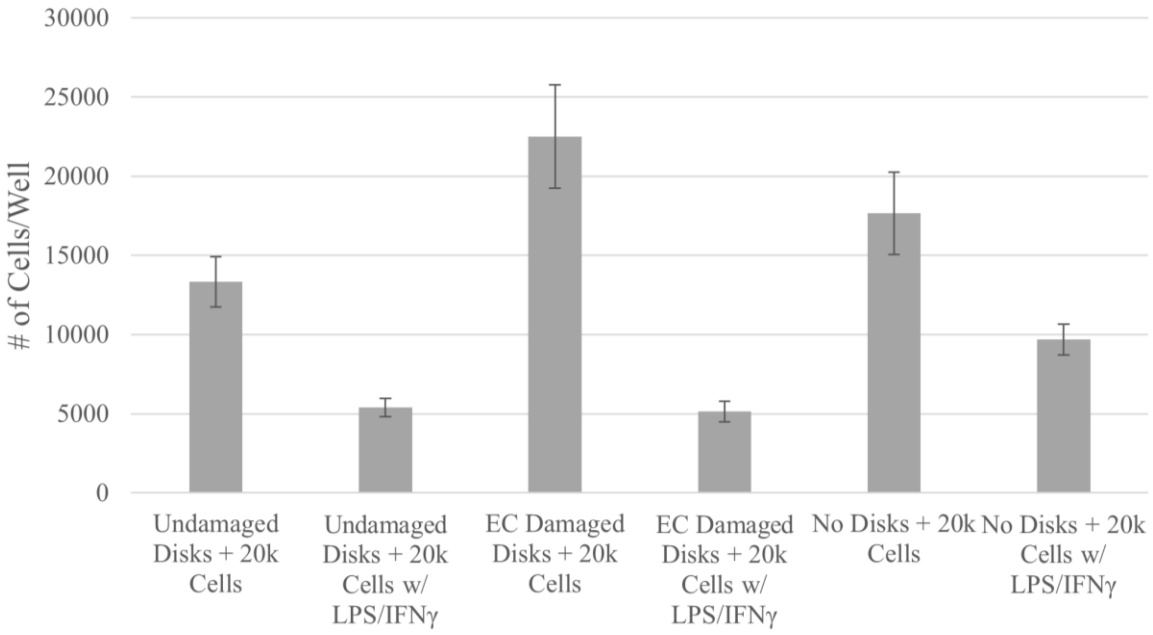

Figure 3-2. Cell Count on Day 30 of the Experiment
Error bars represent ± one standard deviation

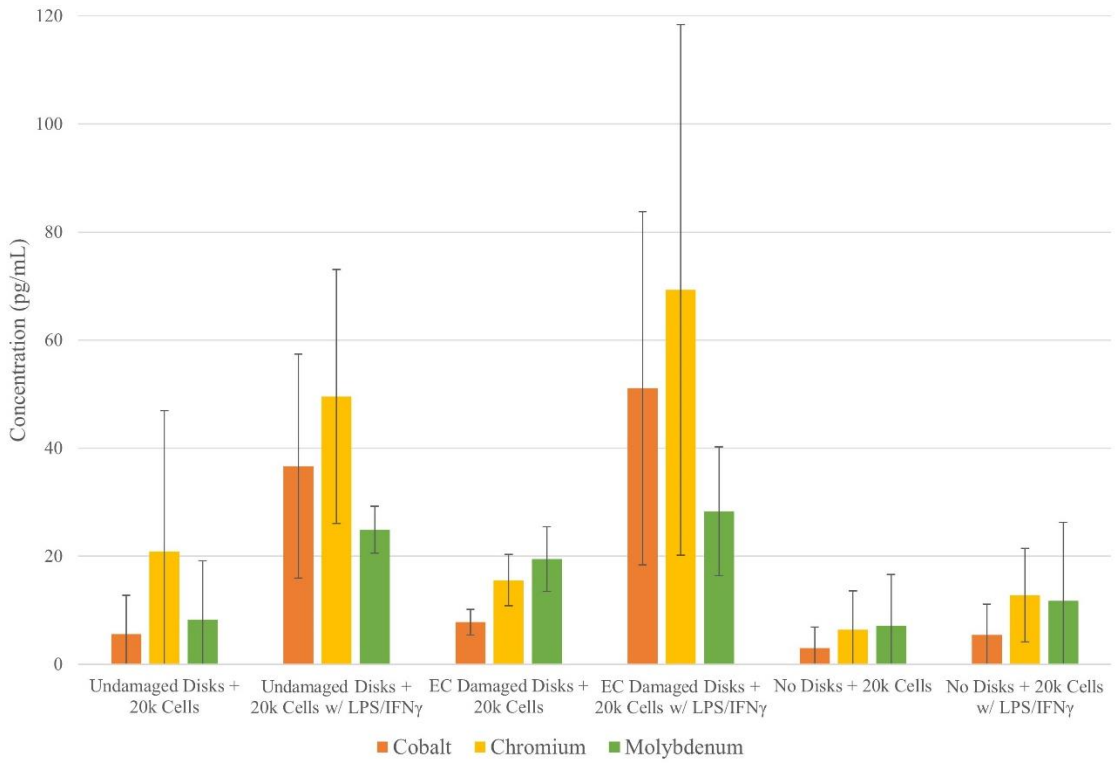

Figure 3-3. Intracellular Metal Concentration per 1000 Cells
Error bars represent ± one standard deviation

significantly higher intracellular Co and Mo concentration in the Undamaged Disks with Activated Cells versus the Undamaged Disks with Standard Cells (P=0.01 and P=0.033). As well as a significantly higher intracellular Co concentration in the EC Damaged Disks with Activated Cells versus the EC Damaged Disks with Standard Cells (P=0.003). However, no significant difference was seen in the intracellular Co, Cr, and Mo concentrations between the Undamaged Disks with Activated Cells versus the EC Damaged Disks with Activated Cells.

SEM and EDS

SEM imaging was able to analyze the surface of the CoCr disks. Visible pitting, resembling ICIC, was seen on the surface of several CoCr disks that were not damaged with an EC device (**Figure 3-4**). SEM images were also able to obtain a microscopic view of the EC damaged areas of the disks (**Figure 3-5**).

EDS Backscatter analysis provided the elemental profile of the CoCr disks for each experimental group (**Figure 3-6)**. Only the CoCr disks that underwent EC damage displayed Nickel on the disk surface. The disks that underwent EC damage also displayed higher average percent weight of Carbon, Oxygen, and Iron compared to the groups with undamaged disks (**Table 3-3** through **3-5**). The EDS backscatter also showed that the groups with EC damaged disks displayed significantly less cobalt, chromium, and molybdenum compared to the groups containing undamaged CoCr disks (**Figure A-1)**. Calculating the Fe/C ratio from the EDS Backscatter percent weight (**Figure 3-7; Table 3-6),** the disks with EC damage had a significantly higher Fe/C ratio compared to the undamaged disks. Showing evidence that EC damage alters the chemical profile of the CoCr disk surface.

Discussion

Metal implants are used in a variety of medical applications including orthopaedic, cardiovascular, neural, and dental. Recent studies have found evidence of direct cellular corrosion to implant surfaces *in vivo*. Inflammatory cells such as macrophages, osteoclasts, and lymphocytes are believed to create an immune response due to the presence of metal ions in the system by attaching to implant surfaces and releasing inflammatory cytokines and ROS. The release of inflammatory cytokines presents a higher inflammatory response while the ROS increases oxidation of the metal alloys and damages the passive oxide layer. The goal of this study was to examine the capability of macrophages corroding the surfaces of ASTM 1537 CoCrMo alloy. A secondary goal of this study was to examine the effects of existing oxide layer damage on macrophage response to the alloy surface. And a third goal of this study was to identify if macrophages were capable of ingesting metal particles from the implant surface by analyzing the inner Co, Cr, and Mo ion concentrations inside the macrophages.

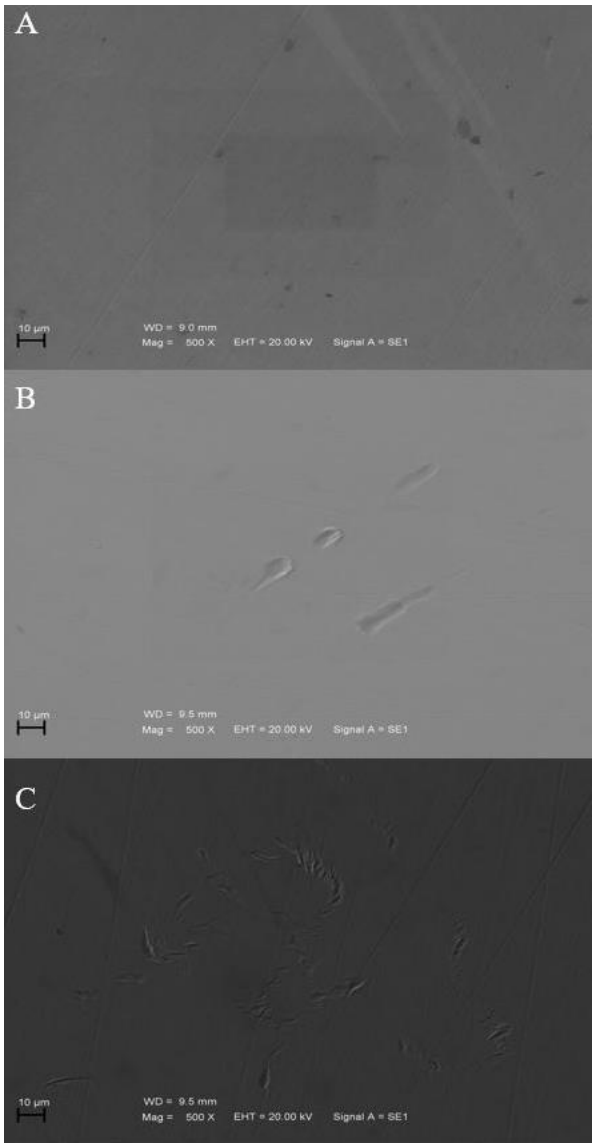

Figure 3-4. SEM Images of the Undamaged CoCr Disks
(A) Undamaged with Medium, (B) Undamaged Disks with 20k Cells and (C) Undamaged Disks with 20k Cells w/ LPS & IFNγ

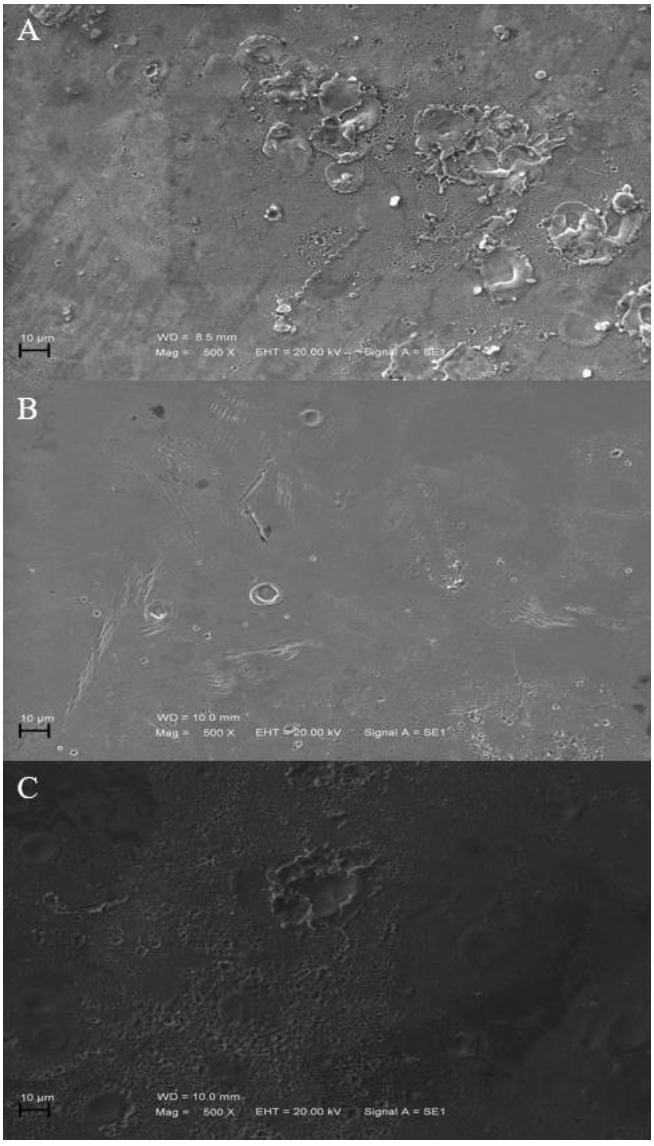

Figure 3-5. SEM Images of the EC Damaged Disks
(A) EC Damaged Disk with Medium and (B) EC Damaged Disks with 20k Cells and (C) EC Damaged Disk with 20k Cells w/ LPS & IFNγ

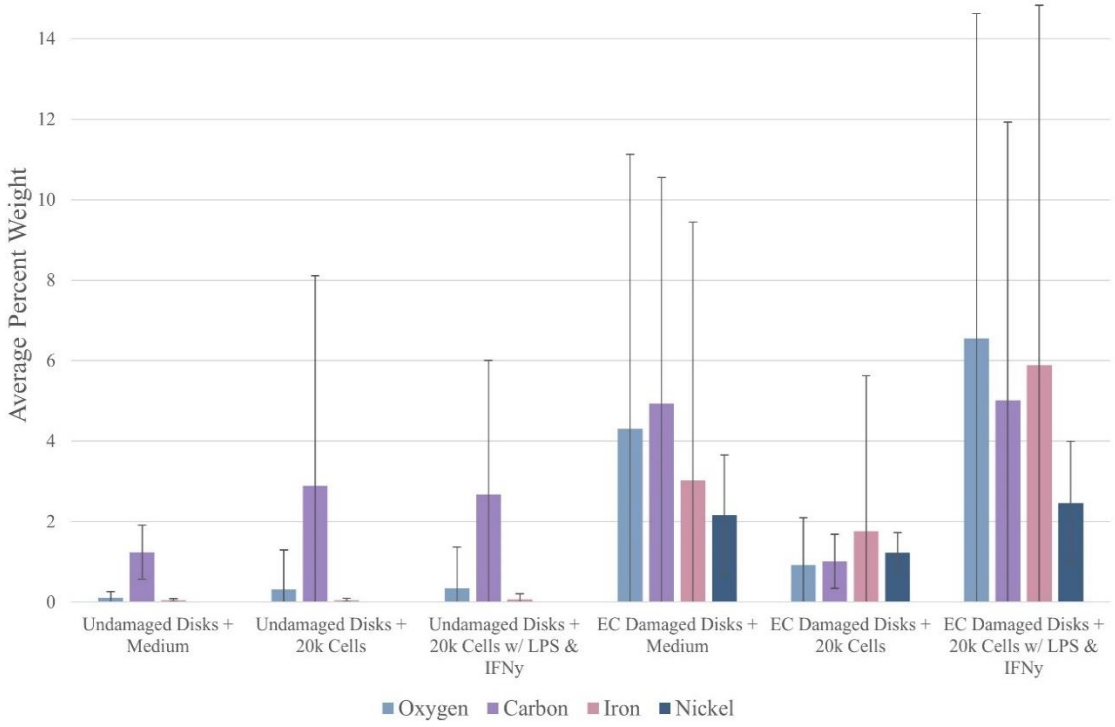

Figure 3-6. Average Percent Weight of Each Element Present on the Surface of the CoCr Disks

Error bars represent ±one standard deviation

Table 3-3. EDS Backscatter Percent Average Weight of Carbon Compared Between Groups

Comparison- Carbon	Difference of Ranks	Q	P
Undamaged Disks + Medium vs. EC Damaged Disks + Medium	320.706	7.321	<0.001
Undamaged Disks + Medium vs. Undamaged Disks + 20k Cells	58.23	1.453	1
Undamaged Disks + Medium vs. EC Damaged Disks + 20k Cells	92.483	1.969	0.735
Undamaged Disks + Medium vs. Undamaged Disks + 20k Cells w/ LPS & IFNy	167.718	4.184	<0.001
Undamaged Disks + Medium vs. EC Damaged Disks + 20k Cells w/ LPS & IFNy	328.93	8.377	<0.001
EC Damaged Disks + Medium vs. Undamaged Disks + 20k Cells	262.476	7.719	<0.001
EC Damaged Disks + Medium vs. EC Damaged Disks + 20k Cells	413.189	9.859	<0.001
EC Damaged Disks + Medium vs. Undamaged Disks + 20k Cells w/ LPS & IFNy	152.988	4.499	<0.001
EC Damaged Disks + Medium vs. EC Damaged Disks + 20k Cells w/ LPS & IFNy	8.224	0.249	1
Undamaged Disks + 20k Cells vs. EC Damaged Disks + 20k Cells	150.713	3.966	0.001
Undamaged Disks + 20k Cells vs. Undamaged Disks + 20k Cells w/ LPS & IFNy	109.488	3.768	0.002
Undamaged Disks + 20k Cells vs. EC Damaged Disks + 20k Cells w/ LPS & IFNy	270.7	9.698	<0.001
EC Damaged Disks + 20k Cells vs. Undamaged Disks + 20k Cells w/ LPS & IFNy	260.201	6.847	<0.001
EC Damaged Disks + 20k Cells vs. EC Damaged Disks + 20k Cells w/ LPS & IFNy	421.413	11.348	<0.001
Undamaged Disks + 20k Cells w/ LPS & IFNy vs. EC Damaged Disks + 20k Cells w/ LPS & IFNy	161.212	5.776	<0.001
Undamaged Disks + Medium vs. EC Damaged Disks + Medium	320.706	7.321	<0.001

*Denotes a statistically significant difference

Table 3-4. EDS Backscatter Percent Average Weight of Oxygen Compared Between Groups

Comparison- Oxygen	Difference of Ranks	Q	P
Undamaged Disks + Medium vs. EC Damaged Disks + Medium	483.743	11.043	<0.001
Undamaged Disks + Medium vs. Undamaged Disks + 20k Cells	19.932	0.497	1
Undamaged Disks + Medium vs. EC Damaged Disks + 20k Cells	302.871	6.447	<0.001
Undamaged Disks + Medium vs. Undamaged Disks + 20k Cells w/ LPS & IFNy	68.904	1.719	1
Undamaged Disks + Medium vs. EC Damaged Disks + 20k Cells w/ LPS & IFNy	525.514	13.384	<0.001
EC Damaged Disks + Medium vs. Undamaged Disks + 20k Cells	463.811	13.64	<0.001
EC Damaged Disks + Medium vs. EC Damaged Disks + 20k Cells	180.872	4.316	<0.001
EC Damaged Disks + Medium vs. Undamaged Disks + 20k Cells w/ LPS & IFNy	414.839	12.2	<0.001
EC Damaged Disks + Medium vs. EC Damaged Disks + 20k Cells w/ LPS & IFNy	41.771	1.265	1
Undamaged Disks + 20k Cells vs. EC Damaged Disks + 20k Cells	282.939	7.445	<0.001
Undamaged Disks + 20k Cells vs. Undamaged Disks + 20k Cells w/ LPS & IFNy	48.972	1.686	1
Undamaged Disks + 20k Cells vs. EC Damaged Disks + 20k Cells w/ LPS & IFNy	505.582	18.113	<0.001
EC Damaged Disks + 20k Cells vs. Undamaged Disks + 20k Cells w/ LPS & IFNy	233.967	6.157	<0.001
EC Damaged Disks + 20k Cells vs. EC Damaged Disks + 20k Cells w/ LPS & IFNy	222.643	5.995	<0.001
Undamaged Disks + 20k Cells w/ LPS & IFNy vs. EC Damaged Disks + 20k Cells w/ LPS & IFNy	456.611	16.359	<0.001

*Denotes a statistically significant difference

Table 3-5. EDS Backscatter Percent Average Weight of Iron Compared Between Groups

Comparison- Iron	Difference of Ranks	Q	P
Undamaged Disks + Medium vs. EC Damaged Disks + Medium	457.758	10.45	<0.001
Undamaged Disks + Medium vs. Undamaged Disks + 20k Cells	10.108	0.252	1
Undamaged Disks + Medium vs. EC Damaged Disks + 20k Cells	354.772	7.552	<0.001
Undamaged Disks + Medium vs. Undamaged Disks + 20k Cells w/ LPS & IFNy	27.337	0.682	1
Undamaged Disks + Medium vs. EC Damaged Disks + 20k Cells w/ LPS & IFNy	525.313	13.379	<0.001
EC Damaged Disks + Medium vs. Undamaged Disks + 20k Cells	447.649	13.165	<0.001
EC Damaged Disks + Medium vs. EC Damaged Disks + 20k Cells	102.985	2.457	0.21
EC Damaged Disks + Medium vs. Undamaged Disks + 20k Cells w/ LPS & IFNy	430.42	12.658	<0.001
EC Damaged Disks + Medium vs. EC Damaged Disks + 20k Cells w/ LPS & IFNy	67.556	2.045	0.613
Undamaged Disks + 20k Cells vs. EC Damaged Disks + 20k Cells	344.664	9.07	<0.001
Undamaged Disks + 20k Cells vs. Undamaged Disks + 20k Cells w/ LPS & IFNy	17.229	0.593	1
Undamaged Disks + 20k Cells vs. EC Damaged Disks + 20k Cells w/ LPS & IFNy	515.205	18.458	<0.001
EC Damaged Disks + 20k Cells vs. Undamaged Disks + 20k Cells w/ LPS & IFNy	327.435	8.616	<0.001
EC Damaged Disks + 20k Cells vs. EC Damaged Disks + 20k Cells w/ LPS & IFNy	170.541	4.592	<0.001
Undamaged Disks + 20k Cells w/ LPS & IFNy vs. EC Damaged Disks + 20k Cells w/ LPS & IFNy	497.976	17.841	<0.001

*Denotes a statistically significant difference

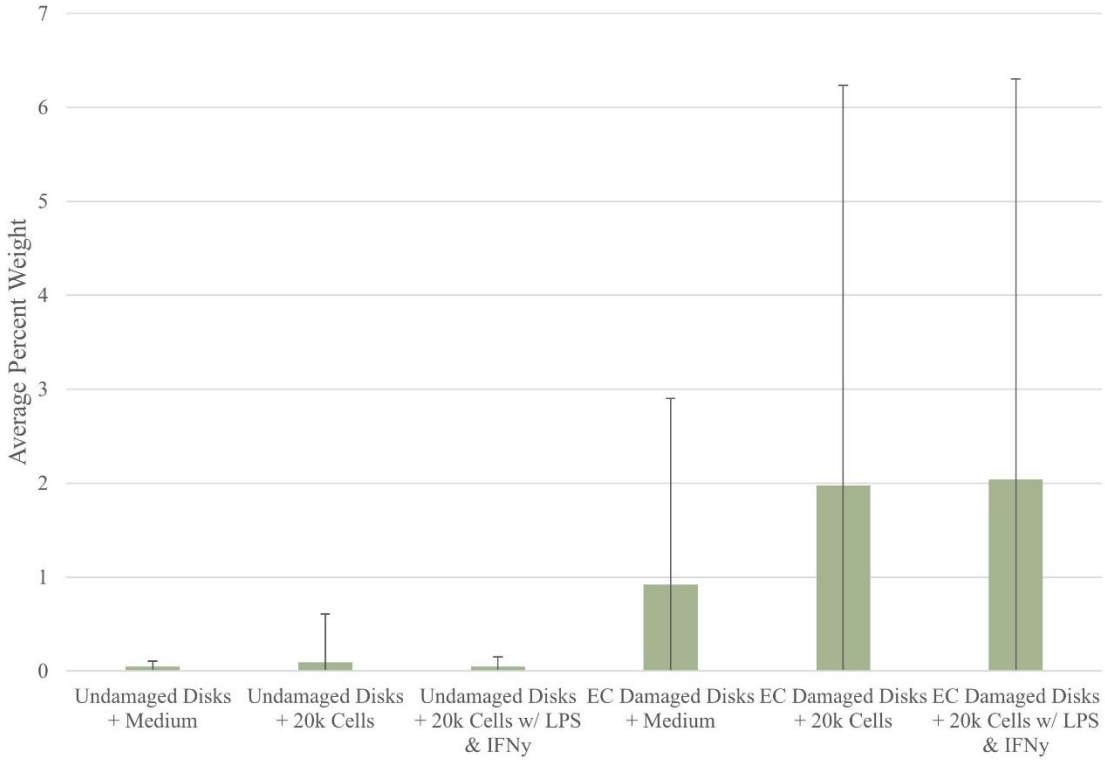

Figure 3-7. Fe/C Backscatter Ratio of the CoCr Disks
Error bars represent ±one standard deviation

Table 3-6. EDS Backscatter Percent Weight of Fe/C Compared Between Groups

Comparison- Fe/C ratio	Difference of Ranks	Q	P
Undamaged Disks + Medium vs. EC Damaged Disks + Medium	338.014	7.574	<0.001
Undamaged Disks + Medium vs. Undamaged Disks + 20k Cells	5.053	0.129	1
Undamaged Disks + Medium vs. EC Damaged Disks + 20k Cells	383.797	8.387	<0.001
Undamaged Disks + Medium vs. Undamaged Disks + 20k Cells w/ LPS & IFNy	31.544	0.808	1
Undamaged Disks + Medium vs. EC Damaged Disks + 20k Cells w/ LPS & IFNy	410.523	10.729	<0.001
EC Damaged Disks + Medium vs. Undamaged Disks + 20k Cells	332.961	9.35	<0.001
EC Damaged Disks + Medium vs. EC Damaged Disks + 20k Cells	45.783	1.068	1
EC Damaged Disks + Medium vs. Undamaged Disks + 20k Cells w/ LPS & IFNy	369.558	10.378	<0.001
EC Damaged Disks + Medium vs. EC Damaged Disks + 20k Cells w/ LPS & IFNy	72.509	2.087	0.554
Undamaged Disks + 20k Cells vs. EC Damaged Disks + 20k Cells	378.744	10.232	<0.001
Undamaged Disks + 20k Cells vs. Undamaged Disks + 20k Cells w/ LPS & IFNy	36.597	1.293	1
Undamaged Disks + 20k Cells vs. EC Damaged Disks + 20k Cells w/ LPS & IFNy	405.47	14.901	<0.001
EC Damaged Disks + 20k Cells vs. Undamaged Disks + 20k Cells w/ LPS & IFNy	415.341	11.22	<0.001
EC Damaged Disks + 20k Cells vs. EC Damaged Disks + 20k Cells w/ LPS & IFNy	26.725	0.738	1
Undamaged Disks + 20k Cells w/ LPS & IFNy vs. EC Damaged Disks + 20k Cells w/ LPS & IFNy	442.067	16.246	<0.001

*Denotes a statistically significant difference

The presence of metal wear debris in the body has been seen to generate an immune response from inflammatory cells. High amounts of Co, Cr, and Mo in the body have been seen to create a variety of physiological issues. In this study, elevated Co metal ion levels were observed in the supernatant fluid of Undamaged Disks with Activated cells and elevated Cr levels were observed in EC Damaged Disks with Standard Cells. Higher levels of Co were seen when comparing Undamaged Disks with Standard Cells versus EC Damaged Disks with Standard Cells and when comparing the Undamaged Disks with Activated Cells versus EC Damaged Disks with Activated Cells. The elevated supernatant fluid metal concentrations provide evidence that the macrophages were capable of attacking the oxide layer of the metal alloy and releasing metal ions into the local environment. While the supernatant fluid did not display drastic differences in the metal ion concentration between the standard and activated cell groups, this could be due to the cells ingesting the metal ions. Elevated metal ion concentrations were observed in the intracellular metal ion concentration of disk groups with activated macrophages. These activated cells groups also saw significantly more cell death than standard cells groups, possibly due to the increased intracellular metal ion concentrations promoting apoptosis. These elevated intracellular metal ion concentrations confirm our hypothesis that the macrophages are capable of ingesting metal ions from the implant surface. However, the clinical significance of these intracellular metal ion concentration values remains unknown. To better understand the ingestion of metal ions by macrophages, a longer *in vitro* experiment should be conducted.

SEM images of the EC damaged disks displayed similar characteristics to damage patterns seen in images from time-of-revision implants. Small cell sized pits were observed on the surface of some undamaged disks that had cultured macrophages. The damage observed on the undamaged disks with cells was not as severe as the damage reported in previous time-of-revision implant retrieval studies [2, 7, 23]. However, this could be due to the experiment's short 30-day *in vitro* timeline. To better understand the damaging effects of macrophages, a longer *in vitro* experiment should be conducted in future studies.

The results from the EDS Backscatter analysis provided evidence supporting differences in the chemical profile between ECIC and ICIC damage areas. Higher levels of Iron and Nickel were seen on disks with EC Damaged Disks compared to the Undamaged Disks. These higher levels could be due to deposition of the Bovie tip on the metal surface during an arcing event but could also be from the grain boundaries in CoCr containing Iron and Nickel. Higher levels of oxygen were observed in the groups containing cells versus their control without cells. These elevated oxygen levels could be due to the release of ROS by macrophages, one of these ROS being hydrogen peroxide. Our EDS results displayed the Fe/C ratio on the EC Damaged Disks was significantly higher than the Fe/C ratio of damage areas seen on the Undamaged Disks. In a study by Heise et al. investigating the occurrence of ICIC on postmortem retrieved TKA implants compared to in vitro EC-induced damage, the specimens intentionally damaged by an EC device displayed a higher Fe/C ratio compared to the ICIC damage areas seen on the necropsy-retrieved implants [6]. This supports our hypothesis that inflammatory cells chemically alter the surface of the metal alloy differently than EC.

CHAPTER 4. CONCLUSION

With the number of TJA increasing every year, it is important to better understand the mechanisms leading to implant failure. The purpose of this thesis was to understand the biological responses and characteristics of TJA implant alloys with and without existing oxide layer damage and provide insight into the clinical significance of damage patterns seen previously in retrieval studies. The studies performed sought out to objectively demonstrate the effects of iatrogenic electrocautery damage and cellular-based corrosion TJA to better understand these damage mechanisms.

Findings from the study discussed in Chapter 2 on EC induced damage of TKA implants confirmed the first two hypotheses defined in this thesis. With the first hypothesis being that there would be differences in the roughness parameters of areas damaged with a MP or BP EC device compared to undamaged implant surface areas. With the second hypothesis being that there would be a difference in the elemental makeup of the MP and BP damaged bearing surfaces compared to undamaged bearing surfaces. The findings from this study demonstrated the adverse effects of EC damage on implant surfaces and its potential effect on wear patterns and metal ion release over the lifetime of the implant. Limitations of this study include the *in vitro* nature of the induced EC damage and that there could still be differences in the local environment imparting less harsh damage than those modeled in this study.

Findings from the study discussed in Chapter 3 on the *in vitro* effects of macrophages on CoCr alloys with and without EC damage confirmed the third hypothesis defined in this thesis. With the third hypothesis being that macrophages cultured on CoCr disks would be capable of ingesting metal ions from the surface of the CoCr disks and thereby affect the surface with a pitting damage to the oxide surface layer. Evidence from the study outlined in Chapter 3 did not support the fourth hypothesis that the macrophages cultured on CoCr disks with existing oxide layer damage would display higher intracellular metal ion concentrations compared to undamaged disks. Findings from this study will crucial insight into the clinical significance of ICIC, and spearhead future research on this form of corrosion. Limitations of this study include the *in vitro* nature of the experiment and the short 30-day period.

CHAPTER 5. FUTURE DIRECTIONS

R21 Grant for Future Studies

While the use of metal alloys for orthopaedic implants have proven useful due to their relatively good biocompatibility and mechanical properties, the release of metal ions to the surrounding tissues leading to possible ALTR and possible local inflammation that may cause eventual implant failure or poor patient reported outcomes may create the need for further research into the causes of implant biologic corrosion. With the number of total joint replacements increasing each year, the need to investigate the factors causing implant-related issues with the local and possibly systemic biological response is paramount. This thesis investigated how EC damage altered the surfaces of different implant types and if inflammatory cells were capable of ingesting metal ions and altering implant surfaces. To better understand implant corrosion, an investigation of how inflammatory cells react to orthopaedic implants with and without varying degrees of EC or fretting damage should be conducted. An NIH R21 grant proposal for such an investigation will be laid out in the remainder of this chapter.

Specific Aims

The overall goal of this future grant proposal is to investigate the cellular mechanisms of implant surface changes to the oxide layer of the implant alloys used for multiple areas of medicine today. Degradation of these implants have been linked to metallosis, adverse local tissue reactions (ALTR), local inflammation, cytotoxicity, and hypersensitivity. The action of inflammatory cells attaching to the metal surface of implants has been known to create a microenvironment of reactive oxygen species (ROS) and Fenton reactions that lead to the disruption of the protective oxide layer and has been termed Inflammatory Cell-Induced Corrosion (ICIC) [5]. This ICIC damage has been seen to leave crevices and pits in the implant surface. This finding, however, closely resembles the damage that occurs following the use of an electrocautery (EC) device. This in turn has caused many to propose that ICIC does not occur and that these pits found on implants in many retrieval databases [12, 18] are actually from surgeons using electrocautery to remove the device. Significant progresses have been made in understanding the response of inflammatory cells to these orthopaedic implants. Our laboratory has also determined from a group of implants recovered at time of necropsy where no electrocautery was utilized to remove the implants that the incidence is much lower (17% versus over 50%) than reported in retrieval databases from surgical revisions [6]. We have also compared the elemental energy dispersion spectrometry of this ICIC versus EC damage is quite different and may be able to define those areas depicting EC versus ICIC types of damage. We have also determined from *in vitro* studies that macrophages are able to ingest and attack areas of EC damage on an implant surface more readily than one that has an intact oxide layer [34]. However, the effects of how inflammatory cells attack and ingest metal particles with varying degrees of oxide layer damage from either iatrogenic or wear-related damage present on the implant surface is

very limited. Understanding how damage to an oxide layer alters inflammatory cell response and metal particle absorption would provide novel insight into a new cause of ALTR and local inflammatory responses to wear. Although cobalt chrome alloys are used mainly in orthopaedic surgery, there are many other surgical specialties that utilize CoCr and other types of susceptible alloys to this type of corrosion (Maxillofascial, Otolaryngology, Plastic and Neurosurgery to name a few). In this proposal, we propose to address this in a comprehensive fashion with the following hypotheses:

- Macrophages cultured on implant alloys without oxide layer damage will show little to no uptake of metallic alloy ions and not interact even when activated with LPS.

- The larger the area of damage whether from fretting or EC damage to an implant alloy surface will allow an exponential increase in the amount of metallic alloy ion uptake by macrophages

These hypotheses will be tested via the following Specific Aims:

Aim 1

Identify how varying degrees of oxide layer damage on CoCr and TiAlV orthopaedic implant alloys influence Inflammatory Cell metal ion uptake, using *in vitro* methods.

Aim 1-Rationale

To better understand to what degree that inflammatory cells are capable of attacking implant oxide layer surfaces, and how EC and fretting/crevice damage alters that degree, we will conduct a 30-day *in vitro* experiment with murine peritoneal macrophages activated with LPS and IFNy. Supernatant fluid will be collected every 5 days and macrophages will be digested on the last day and analyzed for trace amounts of Co, Cr, Mo, Fe, and Nickel using ICP-QQQ-MS as our primary outcome. Secondary outcomes will include surface topography changes to the alloy disks as measured before and after cell culture and medium versus cell content of metal ions as measured after cells are digested at the end of 30 days.

Aim 2

To evaluate the differences in the surface chemical profile of CoCr and TiAlV orthopaedic implant materials after introduction to Inflammatory Cells and varying degrees of oxide layer damage, using Energy Dispersion X-ray Spectroscopy and Scanning Electron Microscopy.

Aim 2-Rationale

Analyzing the chemical profile of the implant material surfaces before and after the *in vitro* experiment will allow us to identify the differences and similarities between ICIC and EC/fretting corrosion in a controlled setting. Previous studies investigating ICIC from implants retrieved at revision have shown higher signs of ECIC than studies investigating ICIC from implants retrieved at necropsy. Microscopic imaging and EDS analysis will help us understand and identify the appropriate corrosion factor.

Research Strategy

Significance

With the number of Total Joint Arthroplasties (TJA) projected to grow to over one million by the year 2030, an investigation into why 20% or more of patients experience long-term pain and/or some functional deficit post-TJA is needed [5, 31, 32]. Previous studies have investigated the occurrence of ICIC and ECIC on implants retrieved from revision and postmortem, but to our knowledge studies looking into recreating ICIC *in vitro* are limited. With the risk of potential revision surgeries being positively correlated with the levels of Co and Cr in the blood, insight into how inflammatory cells can induce implant corrosion is needed [7]. There are also other ways to alter the oxide layer of an alloy. These include fretting and crevice types of corrosion mechanisms which may occur from iatrogenic means or from other unintended contact of retractors and other instruments during implantation or from other mechanical and or wear mechanisms that occur *in vivo*. Knowing that these mechanisms can induce an environment that will open the door to macrophage induced attacks on the implant surface and the release of metal ions into the local environment means that these pathways can be altered or prevented to improve outcomes. This also would invite more improvement in materials whether it be from ceramic coatings or improved solid ceramic implants to negate these effects.

Innovation

While several investigators have been looking into the characteristics and clinical occurrence of ICIC, few investigators have looked into recreating ICIC of orthopaedic implants *in vitro*. This proposal outlines a minimalistic approach to mimic the process of ICIC in vitro allowing for a better understanding of damage mechanisms involved during an inflammatory response to TJA implants. The approaches in this study would provide valuable information important in determining the clinical significance of ICIC and ECIC on the efficacy of TJA implants.

In order to prevent cell death over the course of the experiment and prolong cell exposure to the implant surfaces, fresh growth medium will be supplied to the

macrophages every 12 hours. This frequency ensures that the cultured macrophages have access to fresh nutrients, just as they would *in vivo*.

Approach

Specific Aim 1. Identify how varying degrees of oxide layer damage on CoCr and TiAlV orthopaedic implant alloys influence Inflammatory Cell metal ion uptake, using in vitro methods.

Hypothesis. From our past studies, we have seen that inflammatory cells are capable of altering the surface of CoCr disks by releasing H_2O_2, ingesting metal particles, and also releasing metal particles into their environment. However, with limited sample sizes, it is not known if the degree that these inflammatory cells are intaking metal particles is clinically significant. Nor is it known how varying degrees of EC damage on the implant surface may alter the amount of metal particles being taken up by inflammatory cells, and its clinical significance. To address these questions, in vitro methods would be performed using IC-21 murine peritoneal macrophages activated with LPS and IFNy on disks made of CoCr and Ti6Al4V orthopaedic implant materials. Select disks would also be intentionally damaged using a monopolar EC device at varying power levels to understand the effect of existing damage on the ingestion of metal particles by inflammatory cells. Our hypothesis is that the macrophages will be capable of ingesting metal particles from the CoCr and Ti6Al4V disk surfaces and that the presence of EC damage will increase the inner metal concentrations of the macrophages.

Experimental Approach. IC-21murine peritoneal macrophages with be cultured in a growth medium of RPMI 1640 with 10% Fetal Bovine Serum (Sigma), 1% L-glutamine (Sigma), and 0.13% gentamicin (Sigma). Cells in the activated experimental groups will later be activated with 20 ng/ml LPS and 20ng/mL IFNγ. ASTM 1537 CoCr and Ti6Al4V bar stock will be purchased and cut into disks and polished to the industry standard roughness. Select metal disks will then be taken into the OR and damaged using a monopolar EC device at 30W, 45W, and 60W using a three second hover method 3 mm from the disk surface. Disks will then be cleaned to remove any debris from the EC damaging process and sterilized under UV light.

The metal disks will be placed in a cell plate and the appropriate controls and experimental conditions added. Cells will be allowed to adhere to the disk surfaces for 24 hours. Following the first 24 hours, the growth medium will be changed every 12 hours for 60 days and supernatant fluid collected every 4 days starting on the second day. Following the 60 days, the macrophages will be removed from the disk surfaces and digested using PBS and 1% Triton X100. Supernatant fluid and Digested cells will then be analyzed for trace amounts of Co, Cr, Mo, Fe, and Nickel using ICP-QQQ-MS.

Specific Aim 2. To evaluate the differences in the surface chemical profile of CoCr and TiAlV orthopaedic implant materials after introduction to Inflammatory Cells

and varying degrees of oxide layer damage, using Energy Dispersion X-ray Spectroscopy and Scanning Electron Microscopy.

Hypothesis. Our past explorations have looked into what differences can be seen for the chemical profile of ICIC damage and ECIC damage from implants retrieved postmortem and intentionally damaged implants [3, 6]. Our findings showed that ECIC damage tends to have a significantly higher Fe/C ratio compared to ICIC damage. To better understand how the chemical profiles of ECIC and ICIC differ on orthopaedic implants, the disks undergoing the in vitro study will be analyzed under SEM and EDS to identify the differences in damage patterns and chemical makeup. Our hypothesis is that pitting and crevicing will be evident SEM images of the experimental groups with inflammatory cells. Also, that there will be differences in the amount of Carbon, Oxygen, Iron, and Nickel seen in the EDS backscatter for groups with and without EC damage, and that the Fe/C ratio will increase with increasing EC power.

Experimental Approach. Following the 30-day in vitro experiment disks will be removed from cell culture plates, cleaned in a bath of deionized water and detergent at a ratio of 10:1 for two consecutive 20-minute increments, and ultrasonicated for two 30-minute periods in a water bath with diluted detergent. Disks will then be placed into a SEM to perform detailed microscopic analysis of the disk surfaces. EDS backscatter analysis will determine the percent weight of elements present in any pits or crevices identified during SEM imaging. Comparison of the EDS Backscatter between experimental groups and controls will determine any differences in the chemical profile of ICIC and ECIC damage types.

Conclusions

The outlined proposal would allow for a better understanding into the capabilities of inflammatory cells during their introduction to orthopaedic implant materials. As well as aid in determining the clinical significance of ICIC on orthopaedic implants. While ICIC may not be the only contributing factor in implant corrosion, the inclusion of varying degrees of EC damage will allow for a correlation between both theories of implant corrosion.

LIST OF REFERENCES

1. Sloan, M., A. Premkumar, and N.P. Sheth, *Projected Volume of Primary Total Joint Arthroplasty in the U.S., 2014 to 2030.* J Bone Joint Surg Am, 2018. **100**(17): p. 1455-1460.
2. Gilbert, J.L., et al., *Direct in vivo inflammatory cell-induced corrosion of CoCrMo alloy orthopedic implant surfaces.* J Biomed Mater Res A, 2015. **103**(1): p. 211-23.
3. Miller, K.C., et al., *Electrocautery Induced Damage of Total Knee Implants.* J Arthroplasty, 2021. **36**(3): p. 1126-1132.
4. Sharkey, P.F., et al., *Why are total knee arthroplasties failing today--has anything changed after 10 years?* J Arthroplasty, 2014. **29**(9): p. 1774-8.
5. Liu, Y. and B. Chen, *In vivo corrosion of CoCrMo alloy and biological responses: a review.* Materials Technology, 2017. **33**(2): p. 127-134.
6. Heise, G., et al., *Comparison of Inflammatory Cell-Induced Corrosion and Electrocautery-Induced Damage of Total Knee Implants.* J Long Term Eff Med Implants, 2019. **29**(3): p. 231-238.
7. Di Laura, A., et al., *Clinical relevance of corrosion patterns attributed to inflammatory cell-induced corrosion: A retrieval study.* J Biomed Mater Res B Appl Biomater, 2017. **105**(1): p. 155-164.
8. Williams, D.F., *Specifications for Innovative, Enabling Biomaterials Based on the Principles of Biocompatibility Mechanisms.* Front Bioeng Biotechnol, 2019. **7**: p. 255.
9. Ghasemi-Mobarakeh, L., et al., *Key terminology in biomaterials and biocompatibility.* Current Opinion in Biomedical Engineering, 2019. **10**: p. 45-50.
10. Williams, D.F., *On the mechanisms of biocompatibility.* Biomaterials, 2008. **29**(20): p. 2941-53.
11. Bitar, D. and J. Parvizi, *Biological response to prosthetic debris.* World J Orthop, 2015. **6**(2): p. 172-89.
12. Yuan, N., et al., *Revisiting the concept of inflammatory cell-induced corrosion.* J Biomed Mater Res B Appl Biomater, 2018. **106**(3): p. 1148-1155.
13. Landgraeber, S., et al., *The pathology of orthopedic implant failure is mediated by innate immune system cytokines.* Mediators Inflamm, 2014. **2014**: p. 185150.
14. Hallab, N.J. and J.J. Jacobs, *Chemokines Associated with Pathologic Responses to Orthopedic Implant Debris.* Front Endocrinol (Lausanne), 2017. **8**: p. 5.
15. Hallab, N.J. and J.J. Jacobs, *Biologic Effects of Implant Debris.* Bulletin of the NYU Hospital for Joint Diseases, 2009. **67**: p. 182-8.
16. Purdue, P.E., et al., *The central role of wear debris in periprosthetic osteolysis.* HSS J, 2006. **2**(2): p. 102-13.
17. Neale, S.D., et al., *The effect of particle phagocytosis and metallic wear particles on osteoclast formation and bone resorption in vitro.* J Arthroplasty, 2000. **15**(5): p. 654-62.
18. Cerquiglini, A., et al., *Inflammatory cell-induced corrosion in total knee arthroplasty: A retrieval study.* J Biomed Mater Res B Appl Biomater, 2018. **106**(1): p. 460-467.

19. Hall, D.J., R. Pourzal, and J.J. Jacobs, *What Surgeons Need to Know About Adverse Local Tissue Reaction in Total Hip Arthroplasty.* J Arthroplasty, 2020. **35**(6S): p. S55-S59.
20. Houdek, M.T., et al., *Synovial Fluid Metal Ion Levels are Superior to Blood Metal Ion Levels in Predicting an Adverse Local Tissue Reaction in Failed Total Hip Arthroplasty.* J Arthroplasty, 2021.
21. *IARC Monographs on the Evaluation of Carcinogenic Risks to Humans.* International Agency for Research of Cancer, 1990. **49**.
22. Plummer, D.R., et al., *Diagnosis and Management of Adverse Local Tissue Reactions Secondary to Corrosion at the Head-Neck Junction in Patients With Metal on Polyethylene Bearings.* J Arthroplasty, 2016. **31**(1): p. 264-8.
23. Arnholt, C.M., et al., *Corrosion Damage and Wear Mechanisms in Long-Term Retrieved CoCr Femoral Components for Total Knee Arthroplasty.* J Arthroplasty, 2016. **31**(12): p. 2900-2906.
24. O'Connor, J.L. and D.A. Bloom, *William T. Bovie and electrosurgery.* Surgery, 1996. **119**(4): p. 390-6.
25. Aminimoghaddam, S., R. Pahlevani, and M. Kazemi, *Electrosurgery and clinical applications of electrosurgical devices in gynecologic procedures.* Med J Islam Repub Iran, 2018. **32**: p. 90.
26. Gallagher, K., B. Dhinsa, and J. Miles, *Electrosurgery.* Surgery (Oxford), 2011. **29**(2): p. 70-72.
27. Mullholland, P.H.G.S.N.M.W., *Principles and Practice of Surgery for the Colon, Rectum, and Anus*. 1999, Shock. p. 328.
28. Kubacki, G.W., S. Sivan, and J.L. Gilbert, *Electrosurgery Induced Damage to Ti-6Al-4V and CoCrMo Alloy Surfaces in Orthopedic Implants In Vivo and In Vitro.* J Arthroplasty, 2017. **32**(11): p. 3533-3538.
29. Cordero, I., *Electrosurgical units - how they work and how to use them safely.* Community Eye Health Journal, 2015. **28**(89): p. 15-16.
30. Gibon, E., M.J. Goodman, and S.B. Goodman, *Patient Satisfaction After Total Knee Arthroplasty: A Realistic or Imaginary Goal?* Orthop Clin North Am, 2017. **48**(4): p. 421-431.
31. Beswick, A.D., et al., *What proportion of patients report long-term pain after total hip or knee replacement for osteoarthritis? A systematic review of prospective studies in unselected patients.* BMJ Open, 2012. **2**(1): p. e000435.
32. Wylde, V., et al., *Persistent pain after joint replacement: prevalence, sensory qualities, and postoperative determinants.* Pain, 2011. **152**(3): p. 566-572.
33. Heyse, T.J., et al., *Oxidized zirconium versus cobalt-chromium in TKA: profilometry of retrieved femoral components.* Clin Orthop Relat Res, 2014. **472**(1): p. 277-83.
34. Heise, G., et al., *In vitro effects of macrophages on orthopaedic implant alloys and local release of metallic alloy components.* Bone Joint J, 2020. **102-B**(7_Supple_B): p. 116-121.
35. Xing, Z., et al., *Titanium particles that have undergone phagocytosis by macrophages lose the ability to activate other macrophages.* J Biomed Mater Res B Appl Biomater, 2008. **85**(1): p. 37-41.

APPENDIX. EDS BACKSCATTER OF COBALT, CHROMIUM, AND MOLYBDENUM

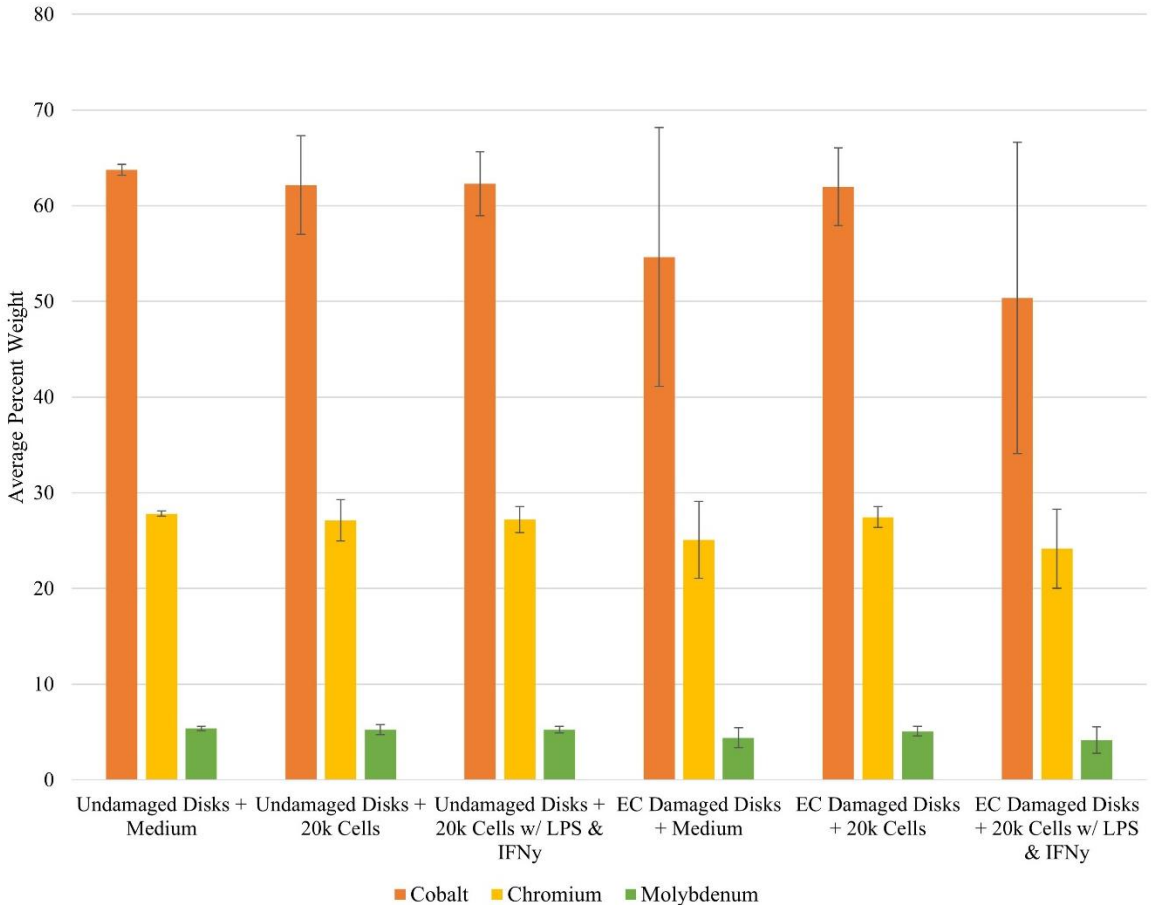

Figure A-1. EDS Backscatter Average Percent Weight of the Cobalt, Chromium and Molybdenum on the CoCr Disks

VITA

Kirsten was born in Sanford, Florida in 1997. She was raised in Lake Mary, Florida where she graduated from Seminole High School in 2015. She attended the University of Central Florida and graduated with a Bachelor of Science degree in Mechanical Engineering in 2019. After graduation, she moved to Memphis, Tennessee to work under Dr. William Mihalko as a graduate research assistant while also obtaining her Master of Science in Biomedical Engineering from the Joint Program in Biomedical Engineering at the University of Tennessee Health Science Center (UTHSC) and the University of Memphis. Kirsten expects to earn her Master of Science Degree in Biomedical Engineering in July 2021.